Secretion systems in Gram-negative bacteria: structural and mechanistic insights

Tiago R. D. Costa, Catarina Felisberto-Rodrigues, Amit Meir*, Marie S. Prevost*, Adam Redzej*, Martina Trokter* and Gabriel Waksman*

Abstract | Bacteria have evolved a remarkable array of sophisticated nanomachines to export various virulence factors across the bacterial cell envelope. In recent years, considerable progress has been made towards elucidating the structural and molecular mechanisms of the six secretion systems (types I–VI) of Gram-negative bacteria, the unique mycobacterial type VII secretion system, the chaperone–usher pathway and the curli secretion machinery. These advances have greatly enhanced our understanding of the complex mechanisms that these macromolecular structures use to deliver proteins and DNA into the extracellular environment or into target cells. In this Review, we explore the structural and mechanistic relationships between these single- and double-membrane-embedded systems, and we briefly discuss how this knowledge can be exploited for the development of new antimicrobial strategies.

Pili
Long appendages that are found on the surface of Gram-negative bacteria and are involved in bacterial attachment, motility and inter-bacterial communication.

Curli
Extracellular amyloid-like protein fibres produced by some bacteria, which are involved in adhesion, biofilm formation and surface colonization.

Institute of Structural and Molecular Biology, University College London and Birkbeck, Malet Street, London WC1E 7HX, UK.
**These authors contributed equally to this work.*
Correspondence to G.W.
e-mails:
g.waksman@ucl.ac.uk;
g.waksman@mail.cryst.bbk.ac.uk
doi:10.1038/nrmicro3456

Bacteria have evolved a wide variety of highly specialized macromolecular nanomachines that secrete a wide range of substrates, including small molecules, proteins and DNA. These substrates have key roles in the response of a bacterium to its environment and also in several physiological processes such as adhesion, pathogenicity, adaptation and survival. Depending on the secretion system, the secreted substrates have three possible fates: they remain associated with the bacterial outer membrane (OM), they are released into the extracellular space, or they are injected into a target cell (either a eukaryotic or bacterial cell)[1].

In Gram-negative bacteria, these machineries can be divided into two categories; those spanning both the inner membrane (IM) and the OM, and those that span the OM only. Single-membrane-spanning transporters in the IM are not discussed here (see REFS 2,3 for excellent reviews on these IM transporters). Five double-membrane-spanning secretion systems have been identified to date and are classified as type I secretion system (T1SS), T2SS, T3SS, T4SS and T6SS (FIG. 1). Those secretion systems that span the OM only include the T5SS and the machineries that assemble cell surface appendages such as type I or P pili and curli (FIG. 2). Finally, mycobacteria, which have a Gram-negative-like cell envelope, encode a T7SS, which is mostly restricted to these bacteria and has not been observed in Gram-negative bacteria[1] (BOX 1).

The secretion of substrates across the bacterial envelope involves either a one-step or two-step secretion mechanism[4]. Apart from the T2SS, all double-membrane-spanning secretion systems (T1SS, T3SS, T4SS and T6SS) use a one-step mechanism, such that substrates are transported directly from the bacterial cytoplasm into the extracellular space or into a target cell. The OM-spanning secretion systems (the T5SS, the chaperone–usher pathway for type I or P pilus biogenesis and the curli secretion system) and the double-membrane-spanning T2SS use a two-step secretion mechanism, whereby substrates are first translocated into the periplasmic space by IM-spanning transporters (such as the SecYEG translocon or the Tat system (twin-arginine translocation system)) and are subsequently transferred to the OM or secreted into the extracellular space by a dedicated OM-spanning secretion system. Most of the OM-spanning and double-membrane-spanning systems exclusively secrete unfolded or partially folded substrates, whereas the T2SS, T6SS and the chaperone–usher pathway can secrete folded or partially folded substrates. None of the seven secretion systems is constitutively active, and it has been suggested that secretion may be triggered by the recognition of host receptors by specialized adhesion molecules called adhesins[1].

In the past decade, a combination of X-ray crystallography and electron microscopy (EM) studies has

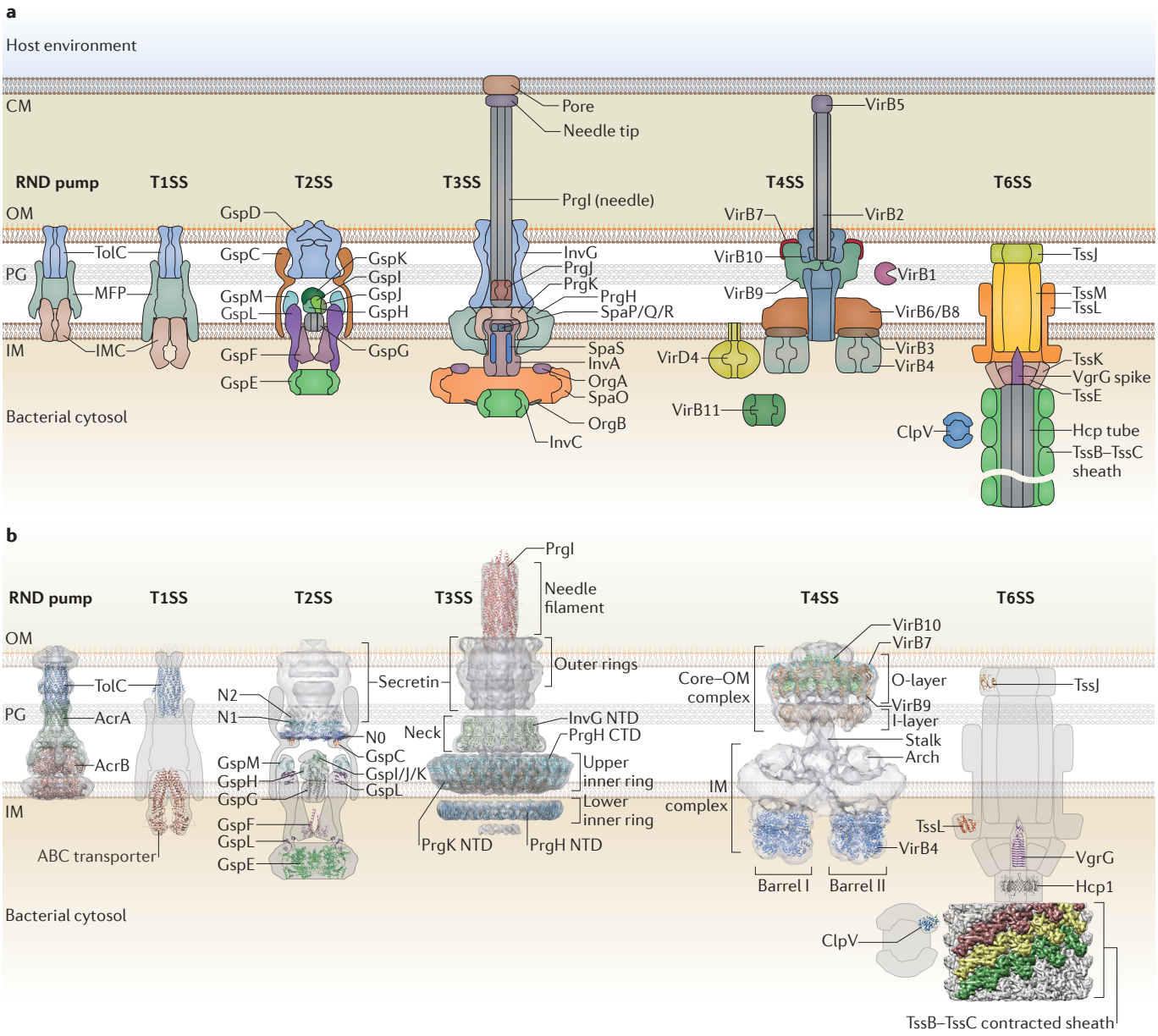

provided near-atomic-resolution details of several of these secretion systems. This multidisciplinary approach has revealed some of the most important structural features of these large complexes and has provided valuable mechanistic insight into substrate recognition and secretion. In this Review, we provide an overview of these recent advances and consider the main functional implications of these findings.

Double-membrane-spanning secretion systems

Tripartite secretion: type I secretion systems and RND efflux pumps. Bacterial T1SSs mediate the secretion of a large variety of protein substrates from the cytoplasm into the extracellular milieu. In pathogenic Gram-negative bacteria, the secreted products, which are diverse in size and function, are often associated with nutrient acquisition (such as HasA, an iron scavenger protein) and virulence (such as the pore-forming protein haemolysin A) [5]. These systems are closely related to the resistance–nodulation–division (RND) family of multidrug efflux pumps in terms of their architectural composition. The RND pumps secrete small exogenous molecules, most of which are antibacterial compounds, out of the cell, thus contributing to antibiotic resistance mechanisms[6]. Both systems form a tripartite double-membrane-spanning channel with an IM component (IMC), a periplasmic adaptor protein (referred to as the membrane fusion protein (MFP)) and TolC, an OM protein channel (FIG. 1a).

In the T1SS, the IMC belongs to the ATP-binding cassette transporter (ABC transporter) family, which is subdivided into 3 groups based on the nature of the IMC amino terminus: groups 1 and 2 contain an additional N-terminal domain (NTD) or 'appendix', called C39 and C39-like domain, respectively, which is involved in substrate recognition; however, this NTD is absent in group 3 (see REF. 5 for a detailed review). T1SS IMCs

SecYEG translocon
Evolutionarily conserved machinery that transports cytosolic proteins through the cytoplasmic membrane of bacteria and archaea and through the membrane of the endoplasmic reticulum in eukaryotic cells.

Tat system
(Twin-arginine-translocation system). A system that transports fully folded protein substrates across the cytoplasmic membrane of bacteria and archaea, and the thylakoid membrane of plant chloroplasts.

Figure 1 | **Structural organization of the secretion systems that span the double membrane of Gram-negative bacteria.** Putative locations of individual protein components are shown schematically in part **a** and the solved structures are shown in part **b**. **a** | Resistance–nodulation–division (RND) pumps and the type I secretion system (T1SS) share an outer membrane (OM) TolC component, a periplasmic membrane fusion protein (MFP) and an inner membrane component (IMC) that supplies energy for transport. The T2SS consists of an OM complex (the dodecameric secretin GspD), a periplasmic pseudopilus (which is composed of the major pseudopilin subunit GspG and the minor pseudopilin subunits GspI, GspJ, GspK and GspH), and an IM platform (GspC, GspF, GspL and GspM) that is tightly associated with the cytoplasmic ATPase GspE. The T3SS cytoplasmic domain includes a hexameric ATPase (InvC) and a sorting platform (SpaO, OrgA and OrgB). The secretin InvG extends from the bacterial OM to the IM base (PrgK, PrgH, SpaP, SpaQ, SpaR, SpaS and InvA), forming a series of protective rings that surround the needle (PrgI). Outside the bacterial cell, the needle tip complex mediates – host cell contact and assists in pore formation. The T4SS is composed of three ATPases (VirD4, VirB4 and VirB11) that, together with VirB3, VirB6 and VirB8, form the IM complex. VirB7, VirB9 and VirB10 form the core–OM complex, with VirB10 extending from the IM to the OM. The conjugative pilus is composed of VirB2 and VirB5. The T6SS TssJ–TssL–TssM membrane complex is connected to the TssB–TssC tail sheath and the haemolysin co-regulated protein (Hcp) inner tube through the baseplate (composed of TssK, TssE, VgrG and probably other proteins). The tail sheath is ~25 times longer than depicted, and its disassembly involves the ClpV ATPase. **b** | An electron microscopy (EM) map of the AcrA–AcrB–TolC RND efflux pump (EM Data Bank (EMDB) identifier: EMD-5915) fitted with X-ray structures of individual components (TolC, Protein Data Bank (PDB) identifier: 2XMN; AcrA, PDB: 2F1M; AcrB, PDB: 4CDI) is shown. For the T1SS, X-ray structures of TolC and the human mitochondrial ABCB10 ATP-binding cassette (ABC) transporter (PDB: 4AYT) are shown. For the T2SS, an EM map of the closed form of the secretin GspD (EMDB: EMD-1763) and X-ray crystal structures of other known components are shown. The crystal structures of the GspD amino-terminal periplasmic domains N0–N1–N2 (PDB: 3EZJ) are also shown. The N0 domain interacts with GspC (PDB: 3OSS). The IM platform is composed of GspL (the periplasmic and cytoplasmic domains of which have been solved (PDB: 2W7V and 2BH1, respectively)), GspM (of which a periplasmic domain structure has been solved (PDB: 1UV7)) and GspF (of which a cytoplasmic domain structure has been solved (PDB: 3C1Q)). GspL contacts the cytoplasmic ATPase GspE (PDB: 4KSR). The pseudopilus is formed by the major pseudopilin GspG (PDB: 3G20) and the minor pseudopilins GspH (PDB: 4DQ9), GspK, GspI and GspJ (the structure of GspK–GspI–GspJ (labelled as Gsp I/J/K) has been solved and is shown (PDB: 3CI0)). For theT3SS, an EM map of the *Salmonella enterica* subsp. *enterica* serovar Typhimurium T3SS needle complex is shown (EMDB: EMD-1875), fitted with atomic structures of the N-terminal domain (NTD) of PrgH (PDB: 3J1W) in the lower inner ring; the carboxy-terminal domain (CTD) of PrgH and the NTD of PrgK (PDB: 2Y9J) in the upper inner ring; the NTD of InvG (PDB: 2Y9K) in the neck; and PrgI (PDB: 2LPZ) in the needle filament. For the T4SS, an EM map of the $T4SS_{3-10}$ complex (EMDB: EMD-2567) is shown, fitted with crystal structures of the VirB4 C-terminal ATPase domain from *Thermoanaerobacter pseudethanolicus* (PDB: 4AG5) and the core–OM complex outer layer (O-layer) (consisting of VirB7 and the CTDs of VirB9 and VirB10) encoded by the *Escherichia coli* pKM101 plasmid (PDB: 3JQO), and with an *in silico* model of the NTD of VirB9 from pKM101 (PDB: 3ZBJ), which together with the NTD of VirB10 forms the core–OM complex inner layer (I-layer). For the T6SS, shown are the crystal structures of TssJ from enteroaggregative *E. coli* (EAEC; PDB: 3RX9), the TssL cytoplasmic domain from EAEC (PDB: 3U66), the PAAR-VgrG spike complex from *Vibrio cholerae* (PDB: 4JIV) and the Hcp1 hexamer from EAEC (PDB: 4HKH). The cryo-EM structure of the contracted TssB–TssC sheath from *V. cholerae* (EMDB: EMD-2524) is also shown, with three out of six protofilaments coloured in green, red and yellow (a schematic representation of the contracted form of the TssB–TssC sheath is shown in FIG. 3e). A schematic representation of the ClpV ATPase is shown to the left of the cryo-EM TssB–TssC structure with the crystal structure of its NTD bound to a TssC peptide (from *V. cholerae* (PDB: 3ZRJ); coloured in blue and green, respectively). CM, cytoplasmic membrane of host cell; PG, peptidoglycan.

function as dimers and recognize a glycine-rich motif (Gly-Gly-X-Gly-X-Asp) that is usually present as a repeat in the carboxyl terminus of its substrates. The system is energized by the hydrolysis of ATP, which is mediated by the C terminus of the IMC[5]. Crystal structures of various ABC transporters suggest an 'alternative-access' mechanism of secretion in which the substrate-binding pocket alternates between a cytoplasm-facing conformation and a periplasm-facing conformation in an ATP-dependent manner[7,8].

In RND pumps, the IMC uses a proton gradient to couple the transport of its substrates to the transport of protons. X-ray crystal structures of the IMC (AcrB) from the AcrA–AcrB–TolC RND pump reveal a trimeric organization in which each AcrB monomer consists of an α-helical transmembrane domain and a large periplasmic domain[9–14]. The protein arrangement of the crystal is such that each AcrB subunit adopts a unique conformation, suggesting that the trimer cycles through three states in which each subunit alternates between the binding, transport and release of the substrate.

MFPs belong to a family of proteins that exhibit sequence similarity with viral fusion proteins. In T1SSs, the MFP component participates in substrate recognition and is either pre-associated with the ABC transporter or is recruited to it following substrate binding[15,16]. The crystal structure of a truncated form of macrolide export protein MacA (the MFP of the MacA–MacB–TolC RND pump), which lacks the membrane proximal domain, shows a homo-hexameric tunnel with an α-hairpin domain (which contains the TolC-binding motif at its tip), together with a β-barrel domain and a lipoyl domain, both of which interact with the IMC[17].

The IMC and MFP components usually recognize only one set of substrates, whereas TolC can associate with several distinct IMC–MFP complexes. TolC is a trimer that forms a β-barrel channel in the OM and a periplasmic α-helical barrel that associates with the MFP. Crystal structures of TolC have shown that the opening of the channel occurs at the periplasmic end of the α-barrel and is triggered by a twisting motion of the α-helices[18–20] (FIG. 1b).

Until recently, the overall structure and organization of the T1SS and of RND pumps were limited to structural data of isolated components or complexes with only two components. In 2014, the cryo-EM structure of the complete AcrA–AcrB–TolC efflux pump, at a resolution of 16 Å, was determined[21]. The efflux pump is composed of a thin drumstick-shaped continuous channel that is approximately 320 Å in length, which is consistent with a double-membrane-spanning structure. The cross-sectional view of the complex reveals a cavity that is between 16 Å and 34 Å in width, from the extracellular side of TolC to the periplasmic side of AcrB. Fitting the X-ray crystal structures of individual components confirmed previous reports that the complex favours a 3/6/3 stoichiometry for AcrB/AcrA/TolC. Finally, TolC adopts an open conformation in the complete structure, which suggests that the opening of TolC occurs on binding of the MFP–IMC complex (FIG. 1b).

From the available structural and functional data, a simple secretion mechanism for the T1SS and for RND pumps has been proposed. In the T1SS, substrates bind to the IMC and are transferred from the cytoplasm, across the IM into the periplasmic cavity of the MFP, using the energy generated from ATP hydrolysis. In

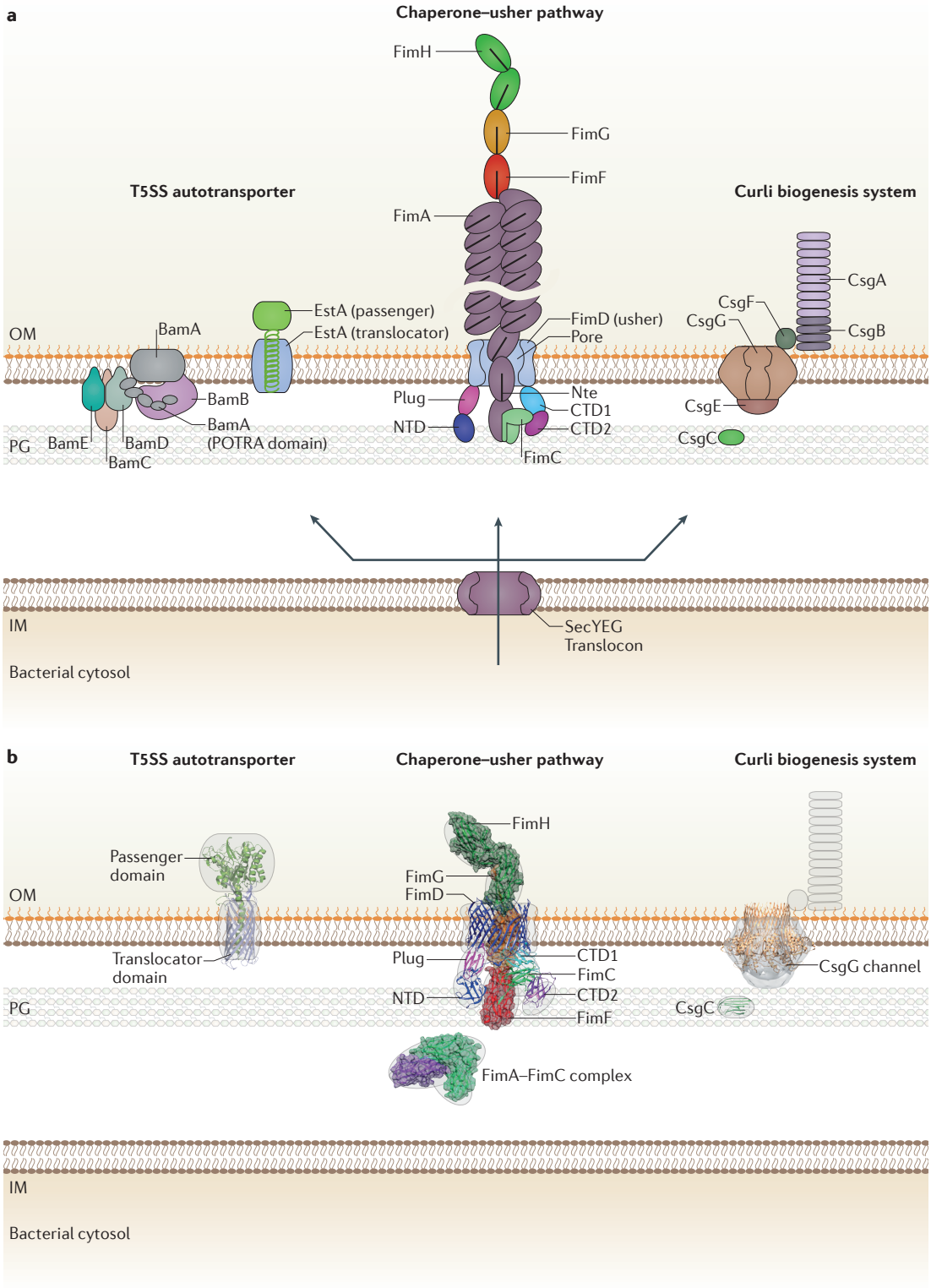

ATP-binding cassette transporter
(ABC transporter). A member of a ubiquitous superfamily of membrane-bound pumps present in all prokaryotes, fungi, plants, yeast and animals. Directional substrate transport across a membrane bilayer is achieved by an ATP-dependent flipping mechanism from an inward- to an outward-facing conformation.

RND pumps, substrates bind to the IMC either in the periplasm or at the inner leaflet of the IM, and they are transferred to the periplasmic cavity of the MFP using the energy generated from proton transport. Binding of the substrate enables the IMC–MFP complex to associate with TolC in the OM. This, in turn, triggers the opening of TolC and the subsequent release of the substrate into the extracellular space (FIG. 3a).

Type II secretion systems. T2SSs are found in a wide variety of pathogenic and non-pathogenic Gram-negative bacteria[22]. The system secretes folded proteins from the periplasm into the extracellular environment, and its substrates include various hydrolysing enzymes, such as pseudolysin of *Pseudomonas aeruginosa* or pullulanase of *Klebsiella pneumoniae* (that are important for bacterial survival and growth in a host or in an

◀ Figure 2 | **Structural organization of the secretion systems that span the outer membrane of Gram-negative bacteria.** Putative locations of individual protein components are shown schematically in part **a**, and the solved structures are shown in part **b**. **a** | The type V secretion system (T5SS) autotransporter (type Va) carboxy-terminal domain (CTD) (the EstA translocator) is inserted into the outer membrane (OM) as a β-barrel, whereas the amino-terminal domain (NTD) of the protein (the EstA passenger) is exposed to the extracellular space after translocation through the β-barrel. The Bam complex (BamA–BamB–BamC–BamD–BamE) is shown as it is involved in the insertion of the EstA translocator domain into the OM and is also possibly involved in secretion of the EstA passenger domain. In the chaperone–usher pathway, a type I pilus is shown, with the subunits FimH, FimG and FimF forming the tip (known as the fibrillum), and ~1,000 FimA subunits forming a thick rod. The usher (which is composed of FimD) contains a pore, plug, NTD, CTD1 and CTD2. The penultimate FimA subunit traverses the pore, whereas the final FimA subunit is on the periplasmic side of the pore and is still bound to the FimC chaperone. In the curli biogenesis system, the secretion channel in the OM is composed of the protein CsgG and is capped on the periplasmic side by the protein CsgE. The minor curli subunit CsgB anchors the major curli subunit CsgA to the OM and nucleates its polymerization. The secretion process is mediated by the two accessory proteins CsgF and CsgC. **b** | The T5SS EstA autotransporter (type Va) of *Pseudomonas aeruginosa* (Protein Data Bank (PDB) identifier: 3KVN) is composed of the translocator and the passenger domains. Shown here are the X-ray crystal structures of the elongation complex FimD–FimH–FimG–FimF–FimC (PDB: 4J3O) of the chaperone–usher pathway and the next subunit–chaperone complex of FimA–FimC (PDB: 4DWH) to be assembled. Also shown is the X-ray crystal structure of the *Escherichia coli* nonameric CsgG channel (PDB: 4UV3) fitted into an electron microscopy map of the nonameric complex of CsgG–CsgE (EM Data Bank (EMDB) identifier: EMD-2750). The X-ray structure of the accessory protein CsgC (PDB: 2Y2Y) is also shown. IM, inner membrane; Nte, N-terminal flexible extension; PG, peptidoglycan.

Pseudopilus
A short pilus-like periplasmic structure in the type II secretion system (composed of the GspG, GspH, GspI, GspJ and GspK pseudopilins) that is involved in substrate extrusion through the outer membrane channel.

Type IV pilus
(T4P). A surface appendage used by many pathogenic bacteria for surface motility, biofilm formation and adhesion at the initial stages of infection. T4Ps enable directional crawling (twitching motility) by cycles of repeated extension-adhesion and retraction-release movements driven by ATPases.

Pilotins
Outer membrane lipoproteins that are involved in secretin oligomerization, insertion and correct localization in the bacterial outer membrane.

Bitopic
A transmembrane protein that contains only one transmembrane segment.

Polytopic
A transmembrane protein that crosses the lipid bilayer twice or more.

environmental niche) and toxins (such as cholera toxin of *Vibrio cholerae*)[22].

The T2SS is composed of 12–15 components, which are called general secretion pathway (Gsp) proteins in enterotoxigenic *Escherichia coli*, Eps in *V. cholerae* and Xcp in *P. aeruginosa*, to mention but a few (only Gsp-based nomenclature will be used hereafter)[23] (FIG. 1a). The T2SS consists of four parts: an OM complex, a periplasmic pseudopilus, an IM platform and a cytoplasmic ATPase. Some of the T2SS components have been well characterized both structurally and biochemically; however, a structure of the entire system is yet to be determined.

The OM complex is formed by the dodecameric protein GspD, which is also referred to as the T2SS secretin. Homologues of this component are found in T3SSs, type IV pilus (T4P) biogenesis systems and in filamentous phage assembly systems[23]. Individual T2SS secretin subunits are composed of a C-terminal domain (CTD), which forms a channel through the OM, and four periplasmic NTDs called N0, N1, N2 and N3 (REF. 24). The 19 Å cryo-EM reconstruction of the *V. cholerae* T2SS secretin revealed a closed cylindrical structure with an outer diameter of 155 Å and a length of 200 Å[24], into which the crystal structure of the N0–N1–N2 domains could be fitted[24–26] (FIG. 1b). In some species, the secretin is recruited to the OM through interactions with pilotins, such as the lipoprotein GspS[27].

The IM platform comprises at least four membrane proteins: GspC, GspF, GspL and GspM (FIG. 1a). GspC, GspL and GspM are bitopic proteins, whereas GspF is a polytopic membrane protein[28–31]. GspC binds to the periplasmic domains of GspD, thereby connecting the IM platform to the OM complex[32,33] (FIG. 1b). The cytoplasmic ATPase, GspE, is a ring-shaped hexamer that is thought to be recruited to the IM platform through its interaction with GspL and GspF[34–36].

T2SSs contain a pseudopilus, which, in contrast to a fully formed pilus that extends into the extracellular space, remains confined within the periplasm (FIG. 1b). The pseudopilus of the T2SS is composed of one major and four minor pseudopilin subunits, and its overall structure is similar to that of the T4P. The pseudopilins are inserted into the IM by the SecYEG translocon and are later cleaved by the peptidase GspO[23]. The major pseudopilus component GspG remains anchored to the IM by an N-terminal helix until it is extracted from the IM and polymerized into a pseudopilus. Interactions between subunits within the pseudopilus are mostly between N-terminal helices[37]. The minor pseudopilins, GspH, GspI, GspJ and GspK, assemble at the tip of the GspG helical filament to complete the formation of the pseudopilus[37,38].

T2SS substrates are transported to the periplasm as unfolded polypeptides by the SecYEG translocon or as folded proteins by the Tat transporter[22]. The T2SS has been suggested to use ATP hydrolysis both to power the assembly of the periplasmic pseudopilus and to push substrates through the OM channel. As GspL interacts with both GspE (the T2SS ATPase[35]) and GspG (the major pseudopilin), it has been suggested that GspL might couple ATPase function with pseudopilus assembly and disassembly (FIG. 1a). The interaction of the pseudopilus with GspC and GspD facilitates insertion of the substrate into the secretin channel[32], and the substrate is then pushed through the secretin channel by extension of the pseudopilus in a piston-like manner[39]. However, the pseudopilus does not extend into the extracellular space. The mechanism by which contacts between the substrate and the secretin promote the opening of the secretin and the secretion of the substrate remain unclear[24] (FIG. 3b).

The T4P biogenesis apparatus is evolutionarily related to the T2SS, and they share structural and functional features. However, in contrast to the T2SS pseudopilus, the T4P extends through the OM secretin and into the extracellular compartment to promote cell adherence, cell motility and DNA transport. The EM reconstruction of the *Neisseria meningitidis* T4P secretin suggests a distinct arrangement of the N0–N1 domains, along with additional β-domains, which are not found in T2SS secretins[40].

Type III secretion systems. T3SSs are double-membrane-embedded nanomachines that are found in various pathogenic Gram-negative bacterial genera such as *Salmonella*, *Shigella*, *Yersinia* and *Pseudomonas*, and enteropathogenic *Escherichia coli* (EPEC)[41]. These specialized protein delivery machines promote the transfer of bacterial effector proteins to the cytoplasm or the plasma membrane of target eukaryotic cells. Within the host, these effectors modulate or subvert specific host cell functions, thereby promoting bacterial invasion and colonization[42,43]. In this Review, we focus mostly on the *Salmonella enterica* subsp. *enterica* serovar

Box 1 | **Type VII secretion in mycobacteria**

The type VII secretion system (T7SS) is a specialized secretion apparatus that is required for the virulence of mycobacteria, such as *Mycobacterium tuberculosis*. The cell envelope of mycobacteria consists of a plasma membrane (which is equivalent to the inner membrane (IM) of Gram-negative bacteria), a periplasmic space that contains peptidoglycan and arabinogalactan, and a thick, complex outer membrane (OM) that contains a waxy lipid coat of mycolic acids called the mycomembrane[156] (see the figure). In 2003, the first T7SS was identified[157], and it was named ESX-1. This system is encoded by a locus that is deleted in attenuated strains of *Mycobacterium bovis* (bacille Calmette–Guérin (BCG) strains), which are used to vaccinate against tuberculosis. T7SS gene clusters have since been identified in several Gram-positive bacteria, such as *Staphylococcus aureus*, *Listeria monocytogenes* and *Bacillus subtilis*[156].

T7SSs are ~1.5 MDa protein complexes that share a conserved IM and cytosolic apparatus. The core channel is composed of the membrane proteins EccB, EccC, EccD and EccE. EccD is predicted to form the central channel in the IM. EccC possesses an ATPase cytoplasmic domain and has been suggested to function as a coupling component. This core channel complex is associated with the mycosin MycP, a membrane protease that has been implicated in substrate processing[158]. In the cytoplasm, two accessory proteins facilitate substrate secretion: EccA, an ATPase from the AAA+ family[156], and EspG, which binds to the substrate and presumably functions as a chaperone to guide the substrate to the secretion apparatus[159]. Several T7SS substrates have been identified and shown to form heterodimers. Their atomic structures have been resolved (EsxA–EsxB, EsxG–EsxH and PE25–PPE41), but their function remains poorly understood[156]. As the machinery that transfers substrates across the mycobacterial OM has yet to be identified, the overall mechanism of translocation is still unclear.

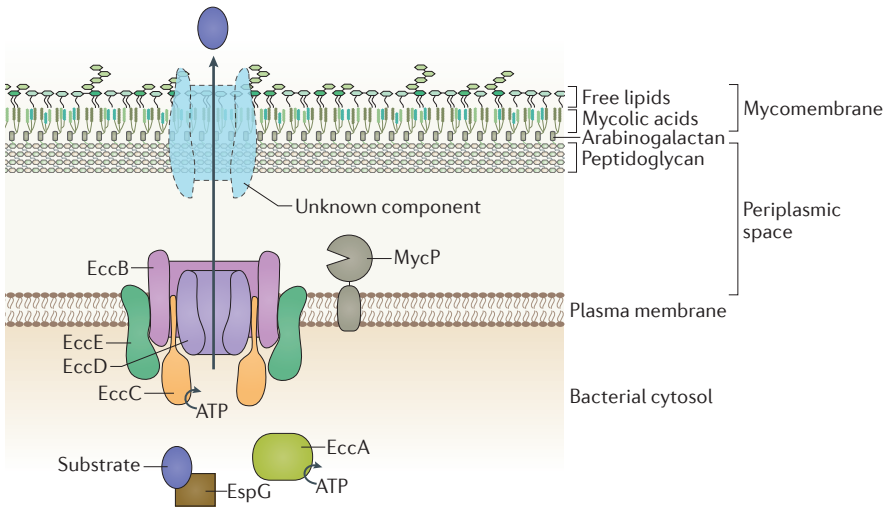

Typhimurium SPI-1 (*Salmonella* pathogenicity island 1) system as a T3SS archetype.

The *S.* Typhimurium T3SS complex was first isolated and visualized by EM more than 15 years ago[44]. The main structural component of the system is a 3.5 MDa multiprotein complex that spans the entire bacterial envelope[44]. This syringe-like structure (also termed the needle complex or injectisome) is composed of approximately 25 proteins that are organized into 2 main substructures: a double-membrane-spanning base that is composed of stacked rings, and a needle-like filament that protrudes from the bacterial surface into the extracellular space[45–47]. In addition, cytosolic components that are essential for substrate recruitment, unfolding and transport associate with the base of the complex following contact with a host cell[48–51] (FIG. 1a).

The base is formed by two concentric inner rings that differ in their diameters (27 nm and 18 nm), which are connected to two outer rings through a structure known as the neck. The two inner rings are inserted into the IM and are composed of at least two proteins, PrgK and PrgH[44,52–54] (FIG. 1b), which are predicted to have single transmembrane domains. In the IM, the NTD of PrgK and the CTD of PrgH localize at the periplasmic side of the IM (these form the 'upper' inner ring), whereas the CTD of PrgK and the NTD of PrgH face the bacterial cytoplasm (these form the 'lower' inner ring) (FIG. 1b). Additional IM components (SpaP, SpaQ, SpaR, SpaS and InvA; see FIG. 1a) have been suggested to associate with the PrgK–PrgH IM channel, and the structures of some of these proteins have been solved[55]. Recently, the structure of a fully assembled nonameric InvA analogue, MxiA (from *Shigella flexneri*), was described, and its location at the base of the needle complex suggested a potential role in controlling secretion[56]. Above the inner rings, the secretin family member InvG constitutes the outer rings (which are inserted into the OM) and the neck that connects to the inner rings[45]. Overall, both inner rings exhibit a 24-fold symmetry and form the largest rings of the complex. Surprisingly, only 15 subunits of InvG form the entirety of the outer rings and the connecting neck. This unusual local asymmetry between the inner rings and outer rings suggests that five subunits of InvG are positioned over eight PrgK–PrgH subunits, implying an overall threefold symmetry for the entire base[45] (FIG. 1b).

The needle-like filament above the base is an extracellular tube-like helical structure that was recently shown to form a secretion conduit from the bacterial OM to

the interior of the host cell[57,58]. This channel, which is composed of more than 100 copies of a single PrgI protein, has a typical length of 30–70 nm and is 10–13 nm in width[46,59]. Structural information, which was obtained by a combination of solid-state nuclear magnetic resonance spectroscopy and Rosetta modelling of *in vitro* assembled needles, showed that the tube has an outer diameter of ~80 Å and that the internal lumen of the tube is ~25 Å in diameter. The structure displayed a right-handed helical torsion with, on average, 5.7 PrgI subunits per turn[60]. Given these dimensions, it would only be possible for fully unfolded substrates to be transported through the narrow secretion channel. A recent cryo-EM structure, in which a substrate was trapped within the secretion channel, demonstrated for the first time that the substrate is indeed unfolded inside the machinery and that the base and the needle-like tube function as an uninterrupted conduit for the substrate[61].

Following contact with a host cell, secretion of the translocator proteins (which form a pore in the host cell membrane) and the effector proteins is triggered by an intricate signalling mechanism that presumably involves conformational changes of the needle filament[62]. The efficient transport of these unfolded T3SS substrates through the polymerized needle filament is controlled by precise secretion signals[43,63,64], which are often encoded within the first 100 residues of the protein and which ensure that secretion proceeds in a hierarchical and coordinated manner[43,64]. T3SS chaperones specifically engage with these regions, ensuring stabilization of the protein (by preventing non-specific interactions) and maintaining the substrate in a secretion-competent state by guiding it to the recognition site of the secretion complex[65] (FIG. 3c). Although much is known about how chaperones engage with and recognize specific T3SS substrates[43,64], how these chaperone–substrate complexes are recognized and transported by the T3SS machinery is poorly understood. However, we now know that these complexes can recognize a group of cytoplasmic proteins (SpaO, OrgA and OrgB; see FIG. 1a) that form a sorting platform at the base of the needle complex[51,66]. The affinity of particular chaperones for this sorting platform might ensure the hierarchical and timely secretion of translocator proteins before effector proteins (FIG. 3c). Once engaged with the sorting platform, substrates are translocated in an ATP-dependent manner through the action of the only known T3SS ATPase InvC.

Type IV secretion systems. T4SSs have the unique ability among secretion systems to mediate the translocation of DNA (in addition to proteins) into bacterial or eukaryotic target cells. T4SSs are found in both Gram-negative and Gram-positive bacteria and also in some archaea[67]. Their most common role is to mediate the conjugation of plasmid DNA; thus, these systems contribute to the spread of plasmid-borne antibiotic resistance genes. As the ability to conjugate is a common bacterial trait, T4SSs are the most ubiquitous secretion systems in nature. In addition, T4SSs are involved in bacterial pathogenesis in a few organisms, and they mediate the secretion of transforming proteins in *Helicobacter pylori*, toxins in *Bordetella pertussis* and other effector proteins required to support an intracellular lifestyle in bacteria such as *Legionella pneumophila*[67].

T4SSs encoded by the Ti plasmid of *Agrobacterium tumefaciens*, together with the T4SSs encoded by the pKM101 and R388 conjugative plasmids of *E. coli*, are the best-characterized T4SSs[67]. They consist of 12 proteins: VirB1, VirB2, VirB3, VirB4, VirB5, VirB6, VirB7, VirB8, VirB9, VirB10, VirB11 and VirD4. Together with VirB3, proteins VirB6, VirB7, VirB8, VirB9 and VirB10 form the scaffold and translocation apparatus[68], whereas VirB2 and VirB5 form the pilus that extends into the extracellular space[69]. VirB1 is a periplasmic lytic transglycosylase that degrades the peptidoglycan layer and is required for pilus biogenesis[69]. The system is powered by three ATPases: VirB4, VirB11 and VirD4 (REF. 69) (FIG. 1a). Other known T4SSs have a similar composition, containing homologues for most or all components[68].

Recently, the structure of the VirB3–VirB10 complex (called $T4SS_{3–10}$) from the R388 plasmid has been determined; this structure provides the first overall view of a T4SS that spans the entire cell envelope[70]. The negative stain EM structure of $T4SS_{3–10}$ shows a core–OM complex that is connected to a bipartite IM complex by a central stalk (FIG. 1b).

The core–OM complex is composed of 14 copies each of VirB7, VirB9 and VirB10, and is similar in structure and composition to the same complex that was previously produced in isolation[71]. It has a distinctive two-layer architecture (called the inner and outer layers), and the two layers are connected by a middle platform[72]. The outer layer is formed by VirB7 and the CTDs of VirB9 and VirB10, whereas the inner layer is formed by the NTDs of VirB9 and VirB10. The crystal structure of the outer layer shows that VirB10 lines the inner side of the core–OM complex and also forms the OM pore, whereas VirB7 and VirB9 wrap around VirB10 (REF. 73) (FIG. 1b). The composition of the middle platform is still unclear[72].

The stalk, the composition of which is unknown, is an elongated structure that connects the core–OM complex and the IM complex. The IM complex comprises VirB3, VirB4, VirB6, VirB8 and the VirB10 N terminus. The cytoplasmic side of the IM complex consists of two barrels that each contain six VirB4 subunits[70] (FIG. 1b). Each VirB4 subunit interacts with a VirB3 subunit, which probably promotes VirB4 insertion into the IM. The IM complex also contains 12 copies of VirB8, 24 copies of VirB6 and 14 copies of the VirB10 N terminus[70]. VirB10 is the only T4SS protein that spans the entire cell envelope and interacts with several different components of the system: VirB7 and VirB9 at the OM and VirB8 at the IM. In addition to this central role, VirB10 is important for substrate transport as it functions as a signal transmitter that relays ATP-driven conformational changes in the cytoplasmic ATPases to the gating of the OM channel[74].

Further insights into the T4SS structure were obtained by the characterization of some of its components in isolation, such as the crystal structures of VirB5 from the pKM101 conjugative plasmid, the periplasmic

Solid-state nuclear magnetic resonance spectroscopy
(Solid-state NMR spectroscopy). A powerful atomic-scale characterization technique applicable to systems that cannot be investigated by either solution NMR or X-ray crystallography, ranging from non-crystalline or poorly crystalline assemblies to protein aggregates or fibrils.

Rosetta modelling
A unified software package for computational protein modelling and functional design.

Conjugative plasmids
Self-transmissible plasmids that possess all of the necessary genes for their own mobilization by conjugation.

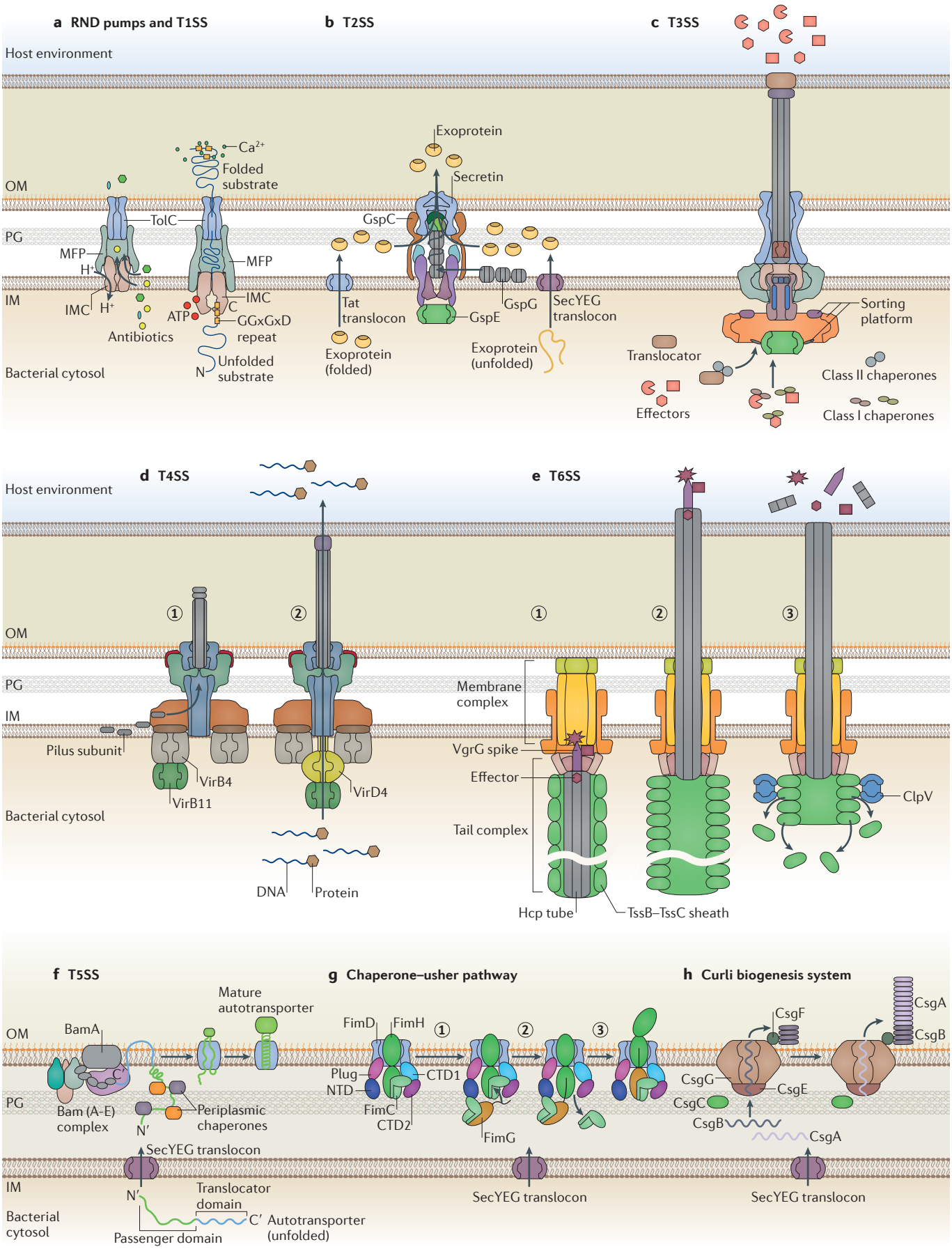

◀ Figure 3 | **Models for the mechanism of substrate secretion in Gram-negative bacteria.** **a** | In resistance–nodulation–division (RND) pumps, antibiotics and small compounds are translocated to the membrane fusion protein (MFP) by the inner membrane component (IMC) using the IM proton gradient, and they are secreted into the extracellular compartment by outer membrane (OM) protein TolC. In type I secretion systems (T1SSs), ATP hydrolysis by the IMC, which in T1SSs is an ATP-binding cassette (ABC) transporter, triggers the transfer of the unfolded substrate to the MFP; TolC secretes the substrate through the OM. **b** | In T2SSs, the general secretion pathway protein GspC recruits the substrate (a folded exoprotein) from the periplasmic space to the secretin. The ATPase activity of GspE is coupled to the assembly of the periplasmic pseudopilus through the IM platform. The pseudopilus pushes the substrate through the secretin channel in a rotary piston-like manner and blocks the channel at the end of the process. **c** | Following T3SS contact with a host cell, the secretion of the translocator proteins before the effector proteins might be determined by the higher affinity of translocator-bound class II chaperones for the sorting platform compared with the lower affinity of the class I chaperones, to which the effectors are bound. Following insertion into the host cell membrane, the translocators form a functional pore that assists the translocation of effectors into the host cell interior. Effector secretion through the T3SS is facilitated by cognate class I chaperones that bind one (class Ia) or multiple (class Ib) effector proteins. **d** | Shown is a schematic representation of the T4SS pathway for pilus biogenesis and substrate translocation. The association of VirB11 with VirB4 promotes pilus subunit assembly (step 1), whereas the association of VirB11 with VirD4 facilitates substrate translocation (step 2). **e** | The T6SS tail complex assembles onto the membrane complex. Effectors are recruited to the spike–tube complex through the extension domains of (and/or non-covalent binding to) VgrG and/or PAAR-repeat proteins and through incorporation into the haemolysin co-regulated protein (Hcp) tube (step 1). An unknown extracellular signal triggers sheath contraction, which leads to the ejection of the spike–tube complex across the target membrane, thereby delivering effector proteins into the cell (step 2). The ATPase ClpV disassembles the contracted TssB–TssC sheath, which enables a new T6SS complex to be reassembled from the released subunits (step 3). Three T6SS core proteins, TssF, TssG and TssA, are not shown here because their roles are unknown. **f** | The unfolded autotransporter of the T5SS is transferred to the periplasm by the SecYEG translocon, where several chaperones stabilize its unfolded structure. In the next stage, the translocator domain is inserted into the OM with the assistance of BamA, where it folds into a β-barrel. The unfolded passenger domain passes through the pore created by the translocator domain and folds into a β-helical structure. **g** | The chaperone–usher pathway. In its resting state, the FimD pore is obstructed by its plug domain. Following activation by FimC–FimH (the first chaperone–pilus subunit complex to be assembled), the plug domain moves into the periplasm, the FimH lectin domain inserts into the FimD pore, and FimC–FimH relocates to the FimD carboxy-terminal domains (CTDs), thereby forming an initiation complex. The next chaperone–pilus subunit complex for assembly, FimC–FimG, is recruited to the FimD amino-terminal domain (NTD) (step 1) placing the N-terminal flexible extension (Nte) of FimG close to the hydrophobic groove of FimH. Next, the donor strand exchange (DSE) process takes place, which results in the FimG Nte invading the groove of FimH, which triggers dissociation of the FimC chaperone from FimH and the FimD CTDs (step 2). The nascent pilus with FimC–FimG at the bottom transfers from the FimD NTD to its CTDs (step 3), freeing up the NTD for binding of the next chaperone–pilus subunit complex in assembly (FimC–FimF). The cycle repeats itself until a fully mature pilus is formed. **h** | In the curli biogenesis system, the CsgG–CsgE complex forms a vestibule in which the unfolded substrate, CsgA, is contained and can only escape by diffusion through the narrow gate of the CsgG channel. CsgA polymerization into a curli fibre is nucleated by the minor curli subunit CsgB. The roles of accessory proteins CsgF and CsgC are still unclear.

domain of VirB8 from *H. pylori* and from *Brucella suis*, and VirB11 from *H. pylori*, as well as the EM reconstruction of isolated VirB4 from the R388 plasmid[75–78]. The crystal structure of the cytoplasmic domain of VirD4 from the R388 plasmid, which is structurally related to the CTD of the ATPase VirB4, has also been solved[79,80]. The conjugative pili are extracellular tubular polymers that establish contact between mating cells and function as channels to transport single-stranded DNA during conjugation[81,82]. In *A. tumefaciens*, the extracellular pilus is formed by the VirB2 pilin polymer, whereas VirB5 is located at the pilus tip, suggesting that it functions in cell-to-cell adhesion[83].

Owing to the absence of VirB11 and VirD4, it is not possible to elucidate the substrate translocation mechanism from the structure of $T4SS_{3-10}$. However, other studies have proposed models for the DNA translocation pathway. First, crosslinking experiments in *A. tumefaciens* have suggested that DNA sequentially contacts VirD4, VirB11, then VirB6 and VirB8 and, finally, VirB9 and VirB2 (REF. 84). Furthermore, although the location of VirB11 remains unclear, it was found that VirB11 from the R388 plasmid interacts with the ATPases VirB4 and VirD4, and that it might regulate pilus biogenesis and substrate translocation depending on which of the two ATPases it associates with[85]. This has led to the proposal that the T4SS switches between two modes: a pilus biogenesis mode, in which VirB11 associates with VirB4, and a substrate-translocation mode, in which VirB11 associates with VirD4[69] (FIG. 3d). The switch between these two modes is proposed to occur when the pilus tip binds to an as-yet-unidentified receptor on recipient cells, which triggers the release of VirB11 from VirB4, thereby enabling it to associate with VirD4 and function in substrate translocation.

Type VI secretion systems. The T6SS is a cell envelope-spanning machine that translocates toxic effector proteins into eukaryotic and prokaryotic cells and has a pivotal role in pathogenesis and bacterial competition[86,87]. The T6SS was functionally defined in 2006 (REF. 88) and is broadly distributed among Proteobacteria[89]. The T6SS is composed of 13 conserved, essential core components and several accessory components[89,90]. Here, we use the 'Tss' nomenclature[86] when naming the T6SS components, whenever possible.

The machinery consists of two main complexes[86]: a membrane complex, which comprises IM proteins that are homologous to components of the T4SS[88,91], and a tail complex that contains components that are evolutionarily related to contractile bacteriophage tails[92]. Growing evidence has established that the T6SS tail complex consists of structural elements that are equivalent to a contractile phage tail: a tail sheath, an inner tube and a baseplate. The T6SS tail complex is anchored to the cell envelope by the membrane complex. The tail sheath is a long tubular structure that is roughly perpendicular to the membrane, and extends deep into the bacterial cell cytoplasm[93] (FIG. 1a).

The minimal T6SS membrane complex is composed of TssJ, TssL and TssM[86]. TssM is an IM protein that connects TssJ, an OM lipoprotein, to TssL, another IM protein[91,94] (FIG. 1a,b). Analogous to phage tail assembly, the T6SS tail tube and sheath are thought to assemble on a platform called the baseplate. Two core components of the T6SS, VgrG and TssE, are homologous to the T4-phage baseplate proteins[92]. TssK is a cytoplasmic subunit that probably connects the TssJ–TssL–TssM membrane complex to the T6SS tail, and it has therefore been proposed to be a component of the T6SS baseplate[95]. The VgrG trimer forms a spike in the centre of the baseplate complex[92,93] (FIG. 1a). It was recently shown

that PAAR-repeat proteins form a conical structure on the VgrG trimer, sharpening the tip of the spike[96] (FIG. 1b). The VgrG spike is thought to function as a nucleation platform for proper assembly of the T6SS tail tube[97] (FIG. 1a). The tail tube comprises polymerized haemolysin co-regulated protein (Hcp), a structural homologue of phage tail tube proteins[92]. *In vitro*, Hcp proteins spontaneously assemble hexameric rings that have an internal diameter of ~40 Å[86,98] (FIG. 1b), whereas, *in vivo*, Hcp hexamers form tubular structures by stacking in a head-to-tail manner[97]. TssB–TssC heterodimers are thought to polymerize around the growing Hcp tube, building the tail sheath[93,97] (FIG. 1a). Sheath polymerization probably stabilizes formation of the Hcp tube. Using time-lapse fluorescence imaging, the T6SS tail sheath of *V. cholerae* was shown to be highly dynamic[93]; the sheaths assemble to lengths that are close to the width of the cell, contract rapidly to about half of their extended length, disassemble and then, finally, reassemble[93].

A 6 Å cryo-EM reconstruction of the *V. cholerae* contracted sheath demonstrated that the sheath is built from 6 TssB–TssC protofilaments[99] (FIG. 1b). The TssB–TssC hexameric rings stack on top of each other with a rotation angle of ~30 degrees, resulting in the 12-tooth cogwheel-like appearance of their cross-sections[93,99,100]. The contracted sheath has an outer diameter of 290 Å, and the central channel is 110 Å in diameter[99]. The structure of a native *V. cholerae* contracted sheath was recently solved by cryo-EM at atomic resolution[101]. The structure shows a core domain, which is assembled from four β-strands that are donated by one TssB and two TssC molecules, that stabilizes the sheath structure. The mechanism of contraction is still not well understood owing to the absence of a high-resolution structure of the extended T6SS sheath.

The mechanism of T6SS secretion is thought to resemble the contraction mechanism of phage tails[93,101]. The current model suggests that, following an unknown extracellular signal, a conformational change in the baseplate complex triggers contraction of the sheath, which leads to the translocation of the inner Hcp tube and of the VgrG–PAAR-repeat proteins out of the cell and across a target membrane[86,87] (FIG. 3e). Effectors are thought to be recruited to the spike–tube complex either as N-terminal or C-terminal extension domains of VgrG and/or the PAAR-repeat proteins, through non-covalent binding to either or both of these proteins[96], by incorporation into the Hcp tube[102] or any combinations thereof (FIG. 3e). Therefore, a single T6SS contraction event might translocate multiple effectors into a target cell[96] (FIG. 3e). The ClpV AAA+ ATPase, which is a core component of the T6SS, is responsible for disassembling the contracted TssB–TssC sheaths, thereby restoring the pool of available sheath subunits[93,100,103] (FIG. 3e). The TssB–TssC conformational change that drives sheath contraction results in exposure of the ClpV recognition motif at the TssC N terminus[99,101,103] (FIG. 1b). As the ClpV recognition motif is presumably buried within the extended sheath, disaggregation of the sheath is restricted to its contracted state. An exception among T6SSs is the *Francisella* T6SS, which lacks a homologue of ClpV and, as a result, does not exhibit highly dynamic behaviour[104]. The atomic structure of the *F. novicida* T6SS sheath was recently determined by cryo-EM, revealing a quaternary structural organization that is different from that of the *V. cholerae* sheath[104]. The functional implications of such differences are, however, unclear.

ClpV recognition motif
A motif present in the amino-terminal domain of TssC that recruits the ATPase ClpV.

Single-membrane-spanning secretion systems

Type V secretion systems. The T5SS, which is also known as the autotransporter system, is unique in that the substrate and its secretion pore are fused to form a single polypeptide. As a result, a single polypeptide can drive its own secretion through the OM, from which the term 'autotransporter' is derived. The T5SS secretes mainly virulence factors but also participates in cell-to-cell adhesion and biofilm formation[105]. Similarly to the T2SS, the chaperone–usher pathway for pilus biogenesis and the curli biogenesis system, the T5SS also requires the SecYEG translocon to transfer an unfolded autotransporter polypeptide through the IM to the periplasm. Autotransporters are composed of a secreted domain, called the 'passenger' domain, that is either semi-unfolded or fully unfolded in the periplasm, and a transmembrane domain (for the OM), which is also called the 'translocator' or 'β–domain' (REF. 106) (FIG. 2a). The translocator domain inserts into the OM as a β-barrel, which enables the secretion of the passenger domain through the pore of the β-barrel. Like other OM transport systems, the process does not require an ATP gradient or a proton gradient, as the energy for transport is derived from the folding of the passenger domain at the pore exit[107].

The T5SS can be divided into five subclasses, denoted a–e[105]. Here, we describe the mechanism of secretion by type Va autotransporters. After transport through the IM, the autotransporter polypeptide is maintained in an unfolded state by dedicated periplasmic chaperones. Recent work has identified the periplasmic chaperone SurA as being sufficient to promote assembly and secretion of the autotransporter[108]. The β-domain of the translocator is subsequently targeted to the Bam complex (a large complex consisting of the integral OM protein BamA and four lipoproteins (BamB, BamC, BamD and BamE)), which assists in the insertion of many β-barrel proteins into the OM[109–112] (FIG. 3f). BamA itself contains a β-barrel domain, the recently obtained structure of which indicates that it is an unstable structure that might open laterally, a feature that could be important in its membrane-insertion function[113,114].

The passenger domain is secreted through the OM from the C terminus[107,115], but its exact mode of secretion is still unclear. One possible mechanism involves the transport of the unfolded passenger domain via a hairpin loop[107]. The domain would then be threaded through the pore to the extracellular milieu, where it would then acquire its folded structure, usually a β-helix. Formation of the β-helix at the pore exit is thought to energize continuous threading of the passenger domain through the pore until secretion is complete. This mechanism is supported by crystal structures[116–118], which show that the linker between the passenger domain and the translocator domain forms an α-helix that traverses

the β-barrel pore (FIG. 2b). These crystal structures support the hypothesis that transport occurs through the β-barrel and suggest that, when hairpin-mediated transport is complete, the linker region between the passenger domain and the β-domain adopts its final α-helical conformation. In the case of some substrates, such as adhesins, the passenger domain remains anchored to the OM, whereas for most substrates it is cleaved by its peptidase domain and released into the extracellular environment.

Several counterarguments suggest that the mechanism of secretion might be more complicated and involves either a direct role for the Bam complex in secretion or involves other protein complexes. First, the β-barrel is only 10 Å wide, which is too narrow for a peptide hairpin to thread through. Second, the hairpin-threading model implies that the two strands of the hairpin must be in an extended conformation, which goes against evidence that the polypeptide inside the β-domain forms an α-helix before completion of secretion[119]. Furthermore, small folded peptides have been shown to be secreted efficiently[120]. A recent study has demonstrated a mechanistic link between β-barrel assembly and the initiation of autotransporter secretion[121]; as the Bam complex mediates β-barrel assembly, this study suggests that it might also have a more active role in secretion. Moreover, a translocation and assembly module (TAM) that promotes efficient secretion of autotransporters has recently been identified[122,123]. Thus, the overall picture emerging from recent work suggests that autotransporters are not autonomous secretion systems but instead involve larger assemblies such as the Bam and TAM complexes that facilitate the coupling of membrane insertion and passenger domain secretion.

The chaperone–usher pathway. The bacterial chaperone–usher pathway is used to assemble and secrete multisubunit appendages called pili or fimbriae, which mediate host cell recognition and attachment and thereby contribute to pathogenicity and biofilm formation[124]. The best-characterized chaperone–usher systems are those for the type I and P pili, which are used by uropathogenic bacteria to colonize and infect the urinary tract[125]. Genes that encode the proteins involved in the assembly and secretion of type I and P pili are located in the *fim* operon and *pap* operon, respectively.

The pilus comprises two parts: a helical rod-like structure that is up to 2 μm long and is composed of several hundred major pilus subunits (FimA for type I pili and PapA for P pili); and a flexible tip that comprises the minor pilus subunits — FimF, FimG and FimH (1 copy each) for the type I pilus, and PapE (5–10 copies), PapF and PapG (1 copy each) and PapK (1 copy) for the P pilus[126,127]. FimH and PapG are at the distal end of their respective pilus tips and possess an N-terminal lectin domain ($FimH_L$ and $PapG_L$) that is crucial for the recognition of and binding to host cell surface receptors[128] (FIG. 2a).

In order to be assembled into a type I or P pilus, all subunits are first secreted via the SecYEG machinery, through the IM and into the periplasm in an unfolded state[129]. The subunits are folded and stabilized by a periplasmic chaperone — FimC for type I pili and PapD for P pili[130]. The resulting chaperone–subunit complexes are then transferred to the site of pilus assembly, an OM protein called an 'usher' (FimD for type I pili and PapC for P pili), which catalyses subunit polymerization and mediates pilus secretion (FIG. 3g).

All pilus subunits, except FimH and PapG, possess two distinct parts: an N-terminal flexible extension (Nte; which is 10–15 residues in length) and an incomplete immunoglobulin-like 'pilin' domain composed of six β-strands (instead of the seven β-strands that are usually found in canonical immunoglobulin-folded proteins)[131]. FimH and PapG have two domains — either $FimH_L$ or $PapG_L$, respectively (mentioned above), and a C-terminal pilin domain, either $FimH_P$ or $PapG_P$, respectively, which is also an incomplete immunoglobulin-like domain with six β-strands. The lack of the seventh β-strand at the C terminus of pilus subunits generates an exposed hydrophobic groove and results in instability of the protein. However, this problem is circumvented either by donor strand complementation (DSC), which involves the donation of a β-strand by the chaperone proteins FimC or PapD (as observed in chaperone–subunit complexes), or by incorporation of the Nte of another subunit (as observed in the assembled pilus). The process by which the chaperone strand is replaced by the Nte of another subunit during pilus biogenesis is called 'donor strand exchange' (DSE) (REF. 131).

The FimD and PapC usher proteins exhibit a complex structure that comprises a 24-stranded β-barrel pore domain that localizes the usher at the OM[132]. In its resting state, the pore of the β-barrel is filled with a plug domain. In addition, the usher possesses two binding sites for chaperone subunits: one is formed by an NTD and the other is formed by two CTDs, CTD1 and CTD2 (REF. 132) (FIG. 2a).

Structural studies of different stages of pilus biogenesis have provided X-ray structures of the initiation complex (which is composed of FimD–FimC–FimH)[132] and the elongation complex (which is composed of FimD–FimH–FimG–FimF–FimC)[133] (FIG. 2b). In the initiation complex, the plug domain has pivoted out of the usher pore into the periplasm. $FimH_L$ is inserted into the usher pore, whereas FimC–$FimH_P$ is bound to CTD1 and CTD2. Interestingly, the docking of the FimC–FimG complex at the NTD of the initiation complex structure shows that the Nte of FimG lies in close proximity to the hydrophobic groove of $FimH_P$. Such a position is optimal for DSE and thus enables invasion of the $FimH_P$ groove by the FimG Nte, leading to displacement of the chaperone that is bound to $FimH_P$ (REF. 132). These findings led to a model of pilus polymerization in which the first chaperone–subunit complex (FimC–FimH) is bound to the usher CTDs and then the next FimC–FimG complex is recruited to the usher NTD, which positions FimG for instant DSE with FimH (FIG. 3g). The Nte of FimG replaces the chaperone β-strand in the hydrophobic groove of $FimH_P$ in a stepwise 'zip-in zip-out' mechanism[134] (FIG. 3g), which leads to the dissociation of the chaperone on $FimH_P$. The

Translocation and assembly module
(TAM). A nanomachine composed of two proteins (the outer membrane protein TamA and the inner membrane TamB subunit), which promotes efficient secretion of autotransporters in Proteobacteria.

Donor strand exchange
(DSE). Chaperone-assisted mechanism of type I pilus assembly in which the stabilizing β-strand that is donated by the chaperone is replaced by the amino-terminal extension of the subunit that is next in assembly.

	T1SS and RND pumps	T2SS	T3SS	T4SS	T5SS	T6SS	OM SS
1940s				Discovery of bacterial conjugation[172]			
1950s							First pilus description[163]
1980s	Discovery of T1SS[169]	Discovery of T2SS[164]	Discovery of T3SS[165]		Discovery of T5SS[170]		Discovery of curli system[136]
1990s	Discovery of RND efflux pumps[168]			Discovery of T4SS[167]			Crystal structure of FimC–FimH[128] PapD–PapK[131] 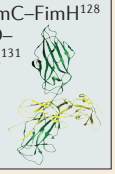
2000s	Crystal structure of TolC[166]  Crystal structure of AcrB[10] 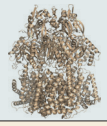 Crystal structure of MacA[17] 	Crystal structure of the minor pseudopilus complex[171] 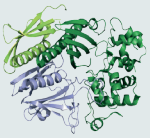	Crystal structure of EscJ (PrjK)[54] 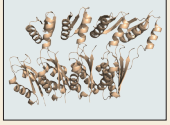 Low-resolution map of the T3SS needle complex[47] 	Cryo-EM structure of the T4SS core complex[71] 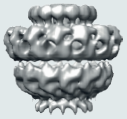 Crystal structure of the T4SS OM complex[73] 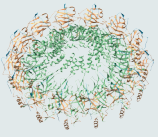	Crystal structure of the translocator domain of the autotransporter NalP[116] 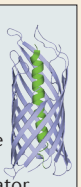	Discovery of T6SS[88] Crystal structure of Hcp[98] 	
2010		EM structure of the secretin[24] 			Crystal structure of EstA[117] 		
2011			Cryo-EM map of the injectiosome[45] 				Crystal structure of FimD/C/H and unbound FimD[132] 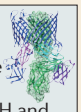
2013					Crystal structure of BamA with 5 POTRA domains[114] 	Crystal structure of PAAR-repeat proteins–VgrG[96] 	Crystal structure of FimD/C/F/G/H[133] 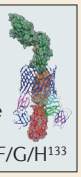
2014	EM structure of the AcrA–AcrB–TolC efflux pump[21] 		EM structure of a substrate-trapped injectisome[61] 	EM structure of the T4SS VirB3–B10 complex[70] 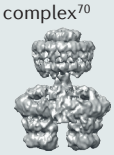		Cryo-EM reconstruction of the TssB/TssC tubule[99] 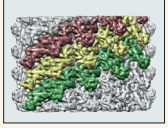	EM structure of CsgG/E[141]  Crystal structure of CsgG[141] 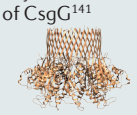

◀ Figure 4 | **Timeline of the discovery of Gram-negative bacterial secretion systems and some of the main structural achievements in the field.** EM, electron microscopy; Hcp, haemolysin co-regulated protein; OM SS, outer membrane secretion system; RND, resistance–nodulation–division; T1SS, type I secretion system.

CTD1- and CTD2-binding site is now vacant so that the nascent pilus can transfer to that site (FIG. 3g), thereby freeing up the usher NTD and making it available for recruitment of the next chaperone–subunit complex in assembly (FimC–FimF). This cycle is then repeated until polymerization stops, which occurs in the P pilus system when the termination subunit PapH binds to the usher. This subunit is unable to undergo DSE and thus remains bound to its chaperone[135]. A termination subunit remains to be identified for the type I pilus assembly system.

Curli. Curli are extracellular protein fibres that belong to the class of functional amyloids, which protect bacteria from hostile environments by contributing to biofilm formation and facilitating interactions with the host immune system[136,137].

Curli fibres are predominantly composed of the major curli subunit protein CsgA, which is translocated through the OM in an unfolded state and is then assembled into fibres with the help of the minor curli subunit CsgB[138] (FIG. 2a). CsgA contains a SecYEG secretion signal sequence and a C-terminal amyloid core domain. The core domain is composed of 5 repeating units R1, R2, R3, R4 and R5 (between 19–24 residues in length), each of which is predicted to form 'β-strand-turn-β-strand' motifs that assemble together to form a cross β-sheet structure that is typical of all amyloids[139,140]. CsgB exhibits a similar domain organization to CsgA, with the exception that the R5 unit lacks residues that are conserved in the other four units. Instead, this unit contains residues that are necessary for the attachment of CsgB to the cell wall. After secretion, CsgB nucleates the polymerization of CsgA subunits into curli fibres.

The curli subunits are secreted by an apparatus that consists of two soluble accessory factors, CsgE and CsgF, and the lipoprotein transporter CsgG, which is located in the OM. The crystal structure of CsgG and the EM structure of the CsgG–CsgE complex have shed light on important aspects of the secretion process[141] (FIG. 2b). CsgG forms an oligomeric structure consisting of 9 subunits, each contributing 4 β-strands to a 36-stranded β-barrel. The periplasmic domains of the CsgG subunits assemble to form a periplasmic vestibule. The region between the transmembrane and periplasmic domains forms a channel constriction of 9 Å in diameter, through which only unfolded extended polypeptides can pass. CsgE forms a nonameric soluble periplasmic adaptor that binds to and plugs the CsgG periplasmic vestibule, thereby creating a large cage below the CsgG secretion channel (FIG. 2b). The size of this cage would be sufficient to accommodate an entire unfolded CsgA subunit. Thus, entrapment and confinement of CsgA within the periplasmic CsgG–CsgE cage creates an entropy gradient across the membrane, leading to extrusion of the CsgA peptide through the CsgG channel. These data suggest that CsgG functions as an ungated, non-selective secretion channel that uses a diffusion-based, entropy-driven transport mechanism similar to that observed in chaperonins[142,143] (FIG. 3h). The roles of CsgC and CsgF in this process are currently unclear; however, it has been suggested that CsgF might be involved in stimulating the assembly of CsgA into fibres on the exterior of the cell[144].

Amyloids
A class of thread-like protein aggregates that self-assemble into insoluble toxic nanofibres. In bacteria, the accumulation of such fibres promotes the formation of a protective biofilm, whereas in humans they are involved in neurodegenerative diseases.

Entropy gradient
An energy gradient produced between two compartments when, in one compartment, the conformational entropy of a peptide or protein is reduced (usually by confinement) while in the other compartment it is not.

Chaperonins
A family of ATP-driven molecular chaperones that form large multisubunit machines to promote protein folding.

Structural relationships between secretion systems

Although each double-membrane-spanning system possesses a unique structure and export mechanism, individual protein components exhibit similarities in structure, shape and/or function. At the OM, both T2SSs and T3SSs contain a ring-like channel called secretin. These proteins have highly similar shapes (ring-like) and structural features (multiple periplasmic domains and a C-terminal transmembrane domain). However, architectural differences within the secretin family are also observed, even between secretion systems of the same type[145]. In the *S.* Typhimurium T3SS, the secretin (InvG) displays a 15-fold symmetrical arrangement, whereas that of *S. flexneri* (MxiD) displays 12-fold symmetry[60]. Even the core–OM complex of T4SSs bears a striking structural resemblance to secretins, except that the secretin-like entity of T4SSs is composed of several proteins, and one of them, VirB10, is extended and inserts into the IM. Another difference is that the T4SS core–OM complex displays 14-fold symmetry. However, recent work on the flagellum biogenesis system, which is evolutionarily related to the T3SS, has shown that subunits of the inner ring shuttle in and out of the system depending on the function that they mediate at a given point in time[146]; this has yet to be demonstrated for outer ring secretin components, but we cannot exclude the possibility that dissimilar symmetries observed within and between OM components might reflect different functional states.

The exact structure of the secretin *trans*-OM domain is still unknown. However, it is intriguing that the OM channel is composed of an α-helical channel in T4SSs; whether this is the case in other secretin-like proteins or complexes is unclear. Nonetheless, all other OM components from single- or double-membrane-spanning secretion systems (with known atomic-resolution structures) form β-barrels in the OM. In single-membrane-spanning T5SSs and the type I pilus and P pilus systems, the translocator domain and usher protein adopt a β-barrel conformation following their integration into the bacterial OM; this is also the case for the OM component TolC of T1SSs. The correct folding and assembly of both autotransporters and usher proteins in the membrane requires the Bam complex, which catalyses the insertion of most β-barrel proteins into the OM[147]. One exception to this is TolC, which does not seem to depend on the Bam complex for OM insertion[105,148].

The presence of dedicated cytoplasmic ATPases (which are usually hexameric) that power substrate secretion is a unique feature of double-membrane-spanning systems. The exception is the T1SS, which uses its dimeric IM component for ATP binding and hydrolysis. The T2SS,

Box 2 | **Bacterial secretion systems as targets for novel antivirulence compounds**

Antibiotics are among the most effective, most successful and least expensive class of drugs that are available for the treatment of disease. However, in recent years, the uncontrolled use (and misuse) of antibiotics has led to the emergence of multidrug-resistant pathogens, which has precipitated an urgent need to develop novel therapies to combat bacterial infections. One approach to reduce the rise of multidrug-resistant strains and to inhibit the spread of resistance determinants is to target virulence factors using small molecules. The inhibition of functional virulence systems would not only render these pathogens harmless but also might facilitate their rapid clearance by the immune system.

Recent advances in our understanding of the molecular and structural biology of Gram-negative bacterial secretion systems have provided unparalleled insight into how bacteria use these systems as virulence factors to cause disease. We are now witnessing intense efforts to translate this knowledge into the design of antivirulence drugs to combat a wide range of infectious diseases.

For example, molecules that target key proteins involved in the type I pilus and P pilus biogenesis systems of uropathogenic *Escherichia coli* have been developed. X-ray structures of the type I pilus adhesin FimH and the P pilus adhesin PapG bound to α-D-mannose and globoside receptors, respectively, have revealed the specific binding sites and interactions of these pili with their cognate host cell surface receptors. Using structure-based approaches, several carbohydrate-based ligands (such as mannose and galabiose derivatives) have been successfully designed to obstruct these host–pathogen interactions. In addition, efforts to target the donor strand exchange reaction between FimH and FimG in the chaperone–usher pathway to prevent pilus polymerization have also been made. Several putative FimH hydrophobic groove binders that reduce complex formation between FimH and the FimG amino-terminal extension have also been identified. Additionally, chemical inhibition of the chaperone that is responsible for the targeting of subunits for polymerization at the usher could impair type I pilus biogenesis. Indeed, a small group of compounds called pilicides, which are characterized by a bicyclic 2-pyridone scaffold, have been identified. These molecules can engage a conserved hydrophobic patch on the rear of the chaperone, thereby perturbing the interaction with the N-terminal periplasmic domain of the usher[154].

Curli biogenesis has also been explored as a target to prevent host colonization and cell invasion. Various molecules (known as curlicides) have been reported to have an effect on polymerization of the major curli subunit CsgA either by disrupting the stability of the protein or by inhibiting its polymerization through inhibition of the nucleation protein, minor curli subunit CsgB[160].

Many classes of chemical compounds have been investigated as potential candidates for type III secretion system (T3SS) inhibition. Although the mechanism of action for most of the disclosed molecules has been elusive, it has been shown that thiazolidinones perturb T3SS needle production in *Salmonella enterica* subsp. *enterica* serovar Typhimurium and *Pseudomonas aeruginosa*. In addition, several benzimidazoles, phenoxyacetamides and salicylidene acylhydrazides display inhibitory activity against T3SSs of several Gram-negative bacteria, such as *P. aeruginosa*, S. Typhimurium, *Chlamydia trachomatis* and *Yersinia pseudotuberculosis*[161]. In *Brucella suis*, VirB8 dimerization is a requirement to assemble a fully functional T4SS and several molecules that target a deep groove opposite the dimerization interface show an inhibitory effect on bacterial proliferation[162].

T3SS and T6SS use a dedicated multimeric ATPase to drive substrate transport through the secretion channel, whereas the T4SS uses three different ATPases to secrete both proteins and DNA. Even more remarkably, at least one of these T4SS hexameric ATPases (VirB4) is present in two copies, giving the system its distinct dipartite shape at the IM. Structural studies of ATPases from the different secretion systems have been extensive, and some of the conformational changes triggered by ATP binding and hydrolysis have been documented[8,34,76,79,80,149–153]; however, studies addressing the mode of action of ATPases in powering substrate transport or apparatus assembly in the context of a fully assembled secretion system are lacking.

The absence of ATP in the periplasmic space imposes a need for the single OM-spanning systems to use alternative energizing mechanisms for transport. In the type I pilus and P pilus biogenesis systems, as well as the T5SS, a common theme has emerged that relies on the formation of low-energy structures at the exit of the secretion channel: in autotransporters of the T5SS, the progressive formation of an extracellular β-helix drives the extrusion of the passenger domain from the β-barrel pore. In the type I pilus and P pilus biogenesis systems, the formation of a super-helical structure of 3.3 FimA or PapA subunits per turn (the 'rod') probably ensures the unidirectionality of transport. Remarkably, in usher-mediated pilus biogenesis, one important step during the incorporation cycle of the chaperone–subunit complexes (specifically, the transfer of the nascent pilus from the usher NTD to the usher CTDs (FIG. 3g)) is assisted by a low-energy path within the usher lumen that forces the subunits to undergo a rotational motion of an amplitude equal to that necessary to bring the nascent pilus from the usher NTD to the usher CTDs[133]. An alternative process is used by the curli system, in which a diffusion-based, entropy-driven transport mechanism is used to assemble amyloid fibres at the bacterial surface[141].

Conclusions and outlook

Over the past 25 years, advances in structural biology have revealed the diverse array of secretion machineries that are assembled by Gram-negative bacteria for the transport of a large portfolio of substrates across the cell envelope (FIG. 4). Although secretion systems are essential for bacteria to adapt to the wide range of environmental conditions that they encounter in nature, their diversity in terms of structures and mechanisms of action poses challenges for the development of vaccines or antivirulence compounds that target these

systems (BOX 2). Nevertheless, structural and molecular advances in the past few years have greatly improved our mechanistic understanding of bacterial secretion systems and have led to the emergence of new drug-design efforts (reviewed in REFS 154,155). In addition to uncovering the different structural features of each system, structural investigations have unravelled the striking structural and functional similarities between system types. It is hoped that we can now exploit these common features to develop new broad-spectrum antibacterial compounds that are specifically designed to minimize the emergence of drug resistance[154,155].

Although astonishing progress has been made, several challenges remain. Does the presence of different types of secretion systems within the same bacterial cell imply a synergistic response towards a host cell? Is the signal induced by contact with a host relayed to the bacterial cell interior by structural changes in the secretion apparatus? If so, which structural components are involved in signal transduction? Is protein unfolding a requirement for substrate progression through all double-membrane-spanning secretion channels? Attempts to trap substrates in the secretion machinery of T3SSs and in the chaperone–usher system have been successful and have shed light on the secretion mechanism used by these systems; these studies need to be extended to other secretion systems, and snapshots of substrate translocation at various stages of the secretion process need to be obtained. Future investigations will also address the energetic mechanism that powers the progression of substrates through the secretion channels and will also aim to identify the structures that are required for substrate recruitment. Finally, atomic-resolution structural details are still lacking for double-membrane-spanning systems, and obtaining these remains one of the most pressing challenges for the future. Such detailed insights are needed to reveal new potential drug targets and to identify new directions for the development of novel antivirulence compounds.

1. Gerlach, R. G. & Hensel, M. Protein secretion systems and adhesins: the molecular armory of Gram-negative pathogens. *Int. J. Med. Microbiol.* **297**, 401–415 (2007).
2. Lycklama a Nijehot, J. A. & Driessen, A. J. M. The bacterial Sec-translocase: structure and mechanism. *Phil. Trans. R. Soc. B* **367**, 1016–1028 (2012).
3. Palmer, T. & Berks, B. C. The twin-arginine translocation (Tat) protein export pathway. *Nature Rev. Microbiol.* **10**, 483–496 (2012).
4. Rego, A. T., Chandran, V. & Waksman, G. Two-step and one-step secretion mechanisms in Gram-negative bacteria: contrasting the type IV secretion system and the chaperone–usher pathway of pilus biogenesis. *Biochem. J.* **425**, 475–488 (2010).
5. Kanonenberg, K., Schwarz, C. K. W. & Schmitt, L. Type I secretion systems — a story of appendices. *Res. Microbiol.* **164**, 596–604 (2013).
6. Piddock, L. J. V. Multidrug-resistance efflux pumps — not just for resistance. *Nature Rev. Microbiol.* **4**, 629–636 (2006).
7. Kadaba, N. S., Kaiser, J. T., Johnson, E., Lee, A. & Rees, D. C. The high-affinity *E. coli* methionine ABC transporter: structure and allosteric regulation. *Science* **321**, 250–253 (2008).
8. Shintre, C. A. *et al.* Structures of ABCB10, a human ATP-binding cassette transporter in apo- and nucleotide-bound states. *Proc. Natl Acad. Sci. USA* **110**, 9710–9715 (2013).
This article describes the molecular mechanism of ABC transporters.
9. Murakami, S., Nakashima, R., Yamashita, E., Matsumoto, T. & Yamaguchi, A. Crystal structures of a multidrug transporter reveal a functionally rotating mechanism. *Nature* **443**, 173–179 (2006).
10. Murakami, S., Nakashima, R., Yamashita, E. & Yamaguchi, A. Crystal structure of bacterial multidrug efflux transporter AcrB. *Nature* **419**, 587–593 (2002).
11. Yu, E. W., McDermott, G., Zgurskaya, H. I., Nikaido, H. & Koshland, D. E. Structural basis of multiple drug-binding capacity of the AcrB multidrug efflux pump. *Science* **300**, 976–980 (2003).
12. Seeger, M. A. Structural asymmetry of AcrB trimer suggests a peristaltic pump mechanism. *Science* **313**, 1295–1298 (2006).
13. Sennhauser, G., Amstutz, P., Briand, C., Storchenegger, O. & Grütter, M. G. Drug export pathway of multidrug exporter AcrB revealed by DARPin inhibitors. *PLoS Biol.* **5**, e7 (2007).
This paper describes the molecular mechanism of transport of the RND inner membrane component.
14. Eicher, T. *et al.* Coupling of remote alternating-access transport mechanisms for protons and substrates in the multidrug efflux pump AcrB. *eLife* **3**, e03145 (2014).
15. Balakrishnan, L., Hughes, C. & Koronakis, V. Substrate-triggered recruitment of the TolC channel-tunnel during type I export of hemolysin by *Escherichia coli*. *J. Mol. Biol.* **313**, 501–510 (2001).
16. Delepelaire, P. Type I secretion in Gram-negative bacteria. *Biochim. Biophys. Acta* **1694**, 149–161 (2004).
17. Yum, S. *et al.* Crystal structure of the periplasmic component of a tripartite macrolide-specific efflux pump. *J. Mol. Biol.* **387**, 1286–1297 (2009).
18. Koronakis, V., Eswaran, J. & Hughes, C. Structure and function of TolC: the bacterial exit duct for proteins and drugs. *Annu. Rev. Biochem.* **73**, 467–489 (2004).
19. Bavro, V. N. *et al.* Assembly and channel opening in a bacterial drug efflux machine. *Mol. Cell* **30**, 114–121 (2008).
This article describes the opening mechanism of TolC.
20. Pei, X. Y. *et al.* Structures of sequential open states in a symmetrical opening transition of the TolC exit duct. *Proc. Natl Acad. Sci. USA* **108**, 2112–2117 (2011).
21. Du, D. *et al.* Structure of the AcrAB–TolC multidrug efflux pump. *Nature* **509**, 512–515 (2014).
This article describes the EM structure of a complete RND pump.
22. Nivaskumar, M. & Francetic, O. Type II secretion system: a magic beanstalk or a protein escalator. *Biochim. Biophys. Acta* **1843**, 1568–1577 (2014).
23. Korotkov, K. V., Sandkvist, M. & Hol, W. G. The type II secretion system: biogenesis, molecular architecture and mechanism. *Nature Rev. Microbiol.* **10**, 336–351 (2012).
24. Reichow, S. L., Korotkov, K. V., Hol, W. G. & Gonen, T. Structure of the cholera toxin secretion channel in its closed state. *Nature Struct. Mol. Biol.* **17**, 1226–1232 (2010).
This study describes the EM map of a T2SS secretin.
25. Korotkov, K. V., Pardon, E., Steyaert, J. & Hol, W. G. Crystal structure of the N-terminal domain of the secretin GspD from ETEC determined with the assistance of a nanobody. *Structure* **17**, 255–265 (2009).
26. Korotkov, K. V., Delarosa, J. R. & Hol, W. G. A dodecameric ring-like structure of the N0 domain of the type II secretin from enterotoxigenic *Escherichia coli*. *J. Struct. Biol.* **183**, 354–362 (2013).
27. Gu, S., Rehman, S., Wang, X., Shevchik, V. E. & Pickersgill, R. W. Structural and functional insights into the pilotin-secretin complex of the type II secretion system. *PLoS Pathog.* **8**, e1002531 (2012).
28. Abendroth, J. *et al.* The three-dimensional structure of the cytoplasmic domains of EpsF from the type 2 secretion system of *Vibrio cholerae*. *J. Struct. Biol.* **166**, 303–315 (2009).
29. Abendroth, J., Bagdasarian, M., Sandkvist, M. & Hol, W. G. The structure of the cytoplasmic domain of EpsL, an inner membrane component of the type II secretion system of *Vibrio cholerae*: an unusual member of the actin-like ATPase superfamily. *J. Mol. Biol.* **344**, 619–633 (2004).
30. Abendroth, J., Murphy, P., Sandkvist, M., Bagdasarian, M. & Hol, W. G. The X-ray structure of the type II secretion system complex formed by the N-terminal domain of EpsE and the cytoplasmic domain of EpsL of *Vibrio cholerae*. *J. Mol. Biol.* **348**, 845–855 (2005).
31. Abendroth, J., Kreger, A. C. & Hol, W. G. The dimer formed by the periplasmic domain of EpsL from the type 2 secretion system of *Vibrio parahaemolyticus*. *J. Struct. Biol.* **168**, 313–322 (2009).
32. Korotkov, K. V. *et al.* Structural and functional studies on the interaction of GspC and GspD in the type II secretion system. *PLoS Pathog.* **7**, e1002228 (2011).
33. McLaughlin, L. S., Haft, R. J. & Forest, K. T. Structural insights into the type II secretion nanomachine. *Curr. Opin. Struct. Biol.* **22**, 208–216 (2012).
34. Lu, C. *et al.* Hexamers of the type II secretion ATPase GspE from *Vibrio cholerae* with increased ATPase activity. *Structure* **21**, 1707–1717 (2013).
35. Gray, M. D., Bagdasarian, M., Hol, W. G. & Sandkvist, M. *In vivo* cross-linking of EpsG to EpsL suggests a role for EpsL as an ATPase-pseudopilin coupling protein in the type II secretion system of *Vibrio cholerae*. *Mol. Microbiol.* **79**, 786–798 (2011).
36. Py, B., Loiseau, L. & Barras, F. An inner membrane platform in the type II secretion machinery of Gram-negative bacteria. *EMBO Rep.* **2**, 244–248 (2001).
37. Campos, M., Nilges, M., Cisneros, D. A. & Francetic, O. Detailed structural and assembly model of the type II secretion pilus from sparse data. *Proc. Natl Acad. Sci. USA* **107**, 13081–13086 (2010).
38. Cisneros, D. A., Pehau-Arnaudet, G. & Francetic, O. Heterologous assembly of type IV pili by a type II secretion system reveals the role of minor pilins in assembly initiation. *Mol. Microbiol.* **86**, 805–818 (2012).
39. Nivaskumar, M. *et al.* Distinct docking and stabilization steps of the pseudopilus conformational transition path suggest rotational assembly of type IV pilus-like fibers. *Structure* **22**, 685–696 (2014).
40. Berry, J. L. *et al.* Structure and assembly of a *trans*-periplasmic channel for type IV pili in *Neisseria meningitidis*. *PLoS Pathog.* **8**, e1002923 (2012).
41. Galan, J. E. & Wolf-Watz, H. Protein delivery into eukaryotic cells by type III secretion machines. *Nature* **444**, 567–573 (2006).
42. Cornelis, G. R. The type III secretion injectisome. *Nature Rev. Microbiol.* **4**, 811–825 (2006).
43. Büttner, D. Protein export according to schedule: architecture, assembly, and regulation of type III secretion systems from plant- and animal-pathogenic bacteria. *Microbiol. Mol. Biol. Rev.* **76**, 262–310 (2012).

44. **Kubori, T.** *et al.* Supramolecular structure of the *Salmonella typhimurium* type III protein secretion system. *Science* **280,** 602–605 (1998).
This study reveals and characterizes the first T3SS isolated from *S.*Typhimurium by EM.
45. Schraidt, O. & Marlovits, T. C. Three-dimensional model of *Salmonella*'s needle complex at subnanometer resolution. *Science* **331**, 1192–1195 (2011).
46. Marlovits, T. C. *et al.* Assembly of the inner rod determines needle length in the type III secretion injectisome. *Nature* **441**, 637–640 (2006).
47. Marlovits, T. C. *et al.* Structural insights into the assembly of the type III secretion needle complex. *Science* **306**, 1040–1042 (2004).
This paper provides the first structural insights into a T3SS needle complex.
48. Kawamoto, A. *et al.* Common and distinct structural features of *Salmonella* injectisome and flagellar basal body. *Sci. Rep.* **3**, 3369 (2013).
49. Eichelberg, K., Ginocchio, C. C. & Galan, J. E. Molecular and functional characterization of the *Salmonella typhimurium* invasion genes *invB* and *invC*: homology of InvC to the F_0F_1 ATPase family of proteins. *J. Bacteriol.* **176**, 4501–4510 (1994).
50. Akeda, Y. & Galán, J. E. Chaperone release and unfolding of substrates in type III secretion. *Nature* **437**, 911–915 (2005).
51. Lara-Tejero, M., Kato, J., Wagner, S., Liu, X. & Galán, J. E. A sorting platform determines the order of protein secretion in bacterial type III systems. *Science* **331**, 1188–1191 (2011).
52. Schraidt, O. *et al.* Topology and organization of the *Salmonella typhimurium* type III secretion needle complex components. *PLoS Pathog.* **6**, e1000824 (2010).
53. Spreter, T. *et al.* A conserved structural motif mediates formation of the periplasmic rings in the type III secretion system. *Nature Struct. Mol. Biol.* **16**, 468–476 (2009).
54. Yip, C. K. *et al.* Structural characterization of the molecular platform for type III secretion system assembly. *Nature* **435**, 702–707 (2005).
55. Worrall, L. J., Lameignere, E. & Strynadka, N. C. Structural overview of the bacterial injectisome. *Curr. Opin. Microbiol.* **14**, 3–8 (2011).
56. Abrusci, P. *et al.* Architecture of the major component of the type III secretion system export apparatus. *Nature Struct. Mol. Biol.* **20**, 99–104 (2013).
57. Kubori, T., Sukhan, A., Aizawa, S. I. & Galán, J. E. Molecular characterization and assembly of the needle complex of the *Salmonella typhimurium* type III protein secretion system. *Proc. Natl Acad. Sci. USA* **97**, 10225–10230 (2000).
58. Kimbrough, T. G. & Miller, S. I. Contribution of *Salmonella typhimurium* type III secretion components to needle complex formation. *Proc. Natl Acad. Sci. USA* **97**, 11008–11013 (2000).
59. Poyraz, O. *et al.* Protein refolding is required for assembly of the type three secretion needle. *Nature Struct. Mol. Biol.* **17**, 788–792 (2010).
60. Loquet, A. *et al.* Atomic model of the type III secretion system needle. *Nature* **486**, 276–279 (2012).
61. Radics, J., Konigsmaier, L. & Marlovits, T. C. Structure of a pathogenic type 3 secretion system in action. *Nature Struct. Mol. Biol.* **21**, 82–87 (2014).
This study describes the first three-dimensional snapshot of a T3SS needle complex in the process of substrate secretion.
62. Blocker, A. J. *et al.* What's the point of the type III secretion system needle? *Proc. Natl Acad. Sci. USA* **105**, 6507–6513 (2008).
63. Izore, T., Job, V. & Dessen, A. Biogenesis, regulation, and targeting of the type III secretion system. *Structure* **19**, 603–612 (2011).
64. Galan, J. E., Lara-Tejero, M., Marlovits, T. C. & Wagner, S. Bacterial type III secretion systems: specialized nanomachines for protein delivery into target cells. *Annu. Rev. Microbiol.* **68**, 415–438 (2014).
65. Parsot, C., Hamiaux, C. & Page, A. L. The various and varying roles of specific chaperones in type III secretion systems. *Curr. Opin. Microbiol.* **6**, 7–14 (2003).
66. Hu, B. *et al.* Visualization of the type III secretion sorting platform of *Shigella flexneri*. *Proc. Natl Acad. Sci. USA* **112**, 1047–1052 (2015).
67. Alvarez-Martinez, C. E. & Christie, P. J. Biological diversity of prokaryotic type IV secretion systems. *Microbiol. Mol. Biol. Rev.* **73**, 775–808 (2009).
68. Christie, P. J., Whitaker, N. & González-Rivera, C. Mechanism and structure of the bacterial type IV secretion systems. *Biochim. Biophys. Acta* **1843**, 1578–1591 (2014).
69. Trokter, M., Felisberto-Rodrigues, C., Christie, P. J. & Waksman, G. Recent advances in the structural and molecular biology of type IV secretion systems. *Curr. Opin. Struct. Biol.* **27**, 16–23 (2014).
70. Low, H. H. *et al.* Structure of a type IV secretion system. *Nature* **508**, 550–553 (2014).
This is the first study to describe the overall architecture of a T4SS.
71. Fronzes, R. *et al.* Structure of a type IV secretion system core complex. *Science* **323**, 266–268 (2009).
This paper describes the assembly, purification and EM structure of the core–OM complex of a T4SS.
72. Rivera-Calzada, A. *et al.* Structure of a bacterial type IV secretion core complex at subnanometre resolution. *EMBO J.* **32**, 1195–1204 (2013).
73. Chandran, V. *et al.* Structure of the outer membrane complex of a type IV secretion system. *Nature* **462**, 1011–1015 (2009).
74. Cascales, E. & Christie, P. J. *Agrobacterium* VirB10, an ATP energy sensor required for type IV secretion. *Proc. Natl Acad. Sci. USA* **101**, 17228–17233 (2004).
75. Terradot, L. *et al.* Structures of two core subunits of the bacterial type IV secretion system, VirB8 from *Brucella suis* and ComB10 from *Helicobacter pylori*. *Proc. Natl Acad. Sci. USA* **102**, 4596–4601 (2005).
76. Savvides, S. N. *et al.* VirB11 ATPases are dynamic hexameric assemblies: new insights into bacterial type IV secretion. *EMBO J.* **22**, 1969–1980 (2003).
77. Pena, A. *et al.* The hexameric structure of a conjugative VirB4 protein ATPase provides new insights for a functional and phylogenetic relationship with DNA translocases. *J. Biol. Chem.* **287**, 39925–39932 (2012).
78. Yeo, H. J., Yuan, Q., Beck, M. R., Baron, C. & Waksman, G. Structural and functional characterization of the VirB5 protein from the type IV secretion system encoded by the conjugative plasmid pKM101. *Proc. Natl Acad. Sci. USA* **100**, 15947–15952 (2003).
79. Gomis-Rüth, F. X. *et al.* The bacterial conjugation protein TrwB resembles ring helicases and F_1-ATPase. *Nature* **409**, 637–641 (2001).
80. Wallden, K. *et al.* Structure of the VirB4 ATPase, alone and bound to the core complex of a type IV secretion system. *Proc. Natl Acad. Sci. USA* **109**, 11348–11353 (2012).
81. Bradley, D. E. Morphological and serological relationships of conjugative pili. *Plasmid* **4**, 155–169 (1980).
82. Durrenberger, M. B., Villiger, W. & Bachi, T. Conjugational junctions: morphology of specific contacts in conjugating *Escherichia coli* bacteria. *J. Struct. Biol.* **107**, 146–156 (1991).
83. Aly, K. A. & Baron, C. The VirB5 protein localizes to the T-pilus tips in *Agrobacterium tumefaciens*. *Microbiology* **153**, 3766–3775 (2007).
84. Cascales, E. & Christie, P. J. Definition of a bacterial type IV secretion pathway for a DNA substrate. *Science* **304**, 1170–1173 (2004).
This study defines the translocation pathway for a DNA substrate through the bacterial T4SS.
85. Ripoll-Rozada, J., Zunzunegui, S., de la Cruz, F., Arechaga, I. & Cabezon, E. Functional interactions of VirB11 traffic ATPases with VirB4 and VirD4 molecular motors in type IV secretion systems. *J. Bacteriol.* **195**, 4195–4201 (2013).
86. Zoued, A. *et al.* Architecture and assembly of the Type VI secretion system. *Biochim. Biophys. Acta* **1843**, 1664–1673 (2014).
87. Ho, B. T., Dong, T. G. & Mekalanos, J. J. A view to a kill: the bacterial type VI secretion system. *Cell Host Microbe* **15**, 9–21 (2014).
88. Pukatzki, S. *et al.* Identification of a conserved bacterial protein secretion system in *Vibrio cholerae* using the *Dictyostelium* host model system. *Proc. Natl Acad. Sci. USA* **103**, 1528–1533 (2006).
89. Boyer, F., Fichant, G., Berthod, J., Vandenbrouck, Y. & Attree, I. Dissecting the bacterial type VI secretion system by a genome wide *in silico* analysis: what can be learned from available microbial genomic resources? *BMC Genomics* **10**, 104 (2009).
90. Zheng, J. & Leung, K. Y. Dissection of a type VI secretion system in *Edwardsiella tarda*. *Mol. Microbiol.* **66**, 1192–1206 (2007).
91. Ma, L. S., Lin, J. S. & Lai, E. M. An IcmF family protein, $ImpL_M$, is an integral inner membrane protein interacting with $ImpK_L$, and its walker a motif is required for type VI secretion system-mediated Hcp secretion in *Agrobacterium tumefaciens*. *J. Bacteriol.* **191**, 4316–4329 (2009).
92. Leiman, P. G. *et al.* Type VI secretion apparatus and phage tail-associated protein complexes share a common evolutionary origin. *Proc. Natl Acad. Sci. USA* **106**, 4154–4159 (2009).
93. Basler, M., Pilhofer, M., Henderson, G. P., Jensen, G. J. & Mekalanos, J. J. Type VI secretion requires a dynamic contractile phage tail-like structure. *Nature* **483**, 182–186 (2012).
This study uses a combination of fluorescence microscopy and electron microscopy to visualize the T6SS in action.
94. Felisberto-Rodrigues, C. *et al.* Towards a structural comprehension of bacterial type VI secretion systems: characterization of the TssJ–TssM complex of an *Escherichia coli* pathovar. *PLoS Pathog.* **7**, e1002386 (2011).
95. Zoued, A. *et al.* TssK is a trimeric cytoplasmic protein interacting with components of both phage-like and membrane anchoring complexes of the type VI secretion system. *J. Biol. Chem.* **288**, 27031–27041 (2013).
96. Shneider, M. M. *et al.* PAAR-repeat proteins sharpen and diversify the type VI secretion system spike. *Nature* **500**, 350–353 (2013).
97. Brunet, Y. R., Hénin, J., Celia, H. & Cascales, E. Type VI secretion and bacteriophage tail tubes share a common assembly pathway. *EMBO Rep.* **15**, 315–321 (2014).
98. Mougous, J. D. *et al.* A virulence locus of *Pseudomonas aeruginosa* encodes a protein secretion apparatus. *Science* **312**, 1526–1530 (2006).
99. Kube, S. *et al.* Structure of the VipA/B type VI secretion complex suggests a contraction-state-specific recycling mechanism. *Cell Rep.* **8**, 20–30 (2014).
100. Bönemann, G., Pietrosiuk, A., Diemand, A., Zentgraf, H. & Mogk, A. Remodelling of VipA/VipB tubules by ClpV-mediated threading is crucial for type VI protein secretion. *EMBO J.* **28**, 315–325 (2009).
101. Kudryashev, M. *et al.* Structure of the type VI secretion system contractile sheath. *Cell* **160**, 952–962 (2015).
102. Silverman, J. M. *et al.* Haemolysin coregulated protein is an exported receptor and chaperone of type VI secretion substrates. *Mol. Cell* **51**, 584–593 (2013).
103. Basler, M. & Mekalanos, J. J. Type 6 secretion dynamics within and between bacterial cells. *Science* **337**, 815 (2012).
104. Clemens, D. L., Ge, P., Lee, B. Y., Horwitz, M. A. & Zhou, Z. H. Atomic structure of T6SS reveals interlaced array essential to function. *Cell* **160**, 940–951 (2015).
105. Leo, J. C., Grin, I. & Linke, D. Type V secretion: mechanism(s) of autotransport through the bacterial outer membrane. *Phil. Trans. R. Soc. B* **367**, 1088–1101 (2012).
106. Leyton, D. L., Rossiter, A. E. & Henderson, I. R. From self sufficiency to dependence: mechanisms and factors important for autotransporter biogenesis. *Nature Rev. Microbiol.* **10**, 213–225 (2012).
107. Junker, M., Besingi, R. N. & Clark, P. L. Vectorial transport and folding of an autotransporter virulence protein during outer membrane secretion. *Mol. Microbiol.* **71**, 1323–1332 (2009).
108. Roman-Hernandez, G., Peterson, J. H. & Bernstein, H. D. Reconstitution of bacterial autotransporter assembly using purified components. *eLife* **3**, e04234 (2014).
109. Voulhoux, R., Bos, M. P., Geurtsen, J., Mols, M. & Tommassen, J. Role of a highly conserved bacterial protein in outer membrane protein assembly. *Science* **299**, 262–265 (2003).
110. Wu, T. *et al.* Identification of a multicomponent complex required for outer membrane biogenesis in *Escherichia coli*. *Cell* **121**, 235–245 (2005).
111. Hagan, C. L., Kim, S. & Kahne, D. Reconstitution of outer membrane protein assembly from purified components. *Science* **328**, 890–892 (2010).
112. Ieva, R., Tian, P., Peterson, J. H. & Bernstein, H. D. Sequential and spatially restricted interactions of assembly factors with an autotransporter β domain. *Proc. Natl Acad. Sci. USA* **108**, E383–E391 (2011).
113. Noinaj, N., Kuszak, A. J., Balusek, C., Gumbart, J. C. & Buchanan, S. K. Lateral opening and exit pore formation are required for BamA function. *Structure* **22**, 1055–1062 (2014).
114. Noinaj, N. *et al.* Structural insight into the biogenesis of β-barrel membrane proteins. *Nature* **501**, 385–390 (2013).

115. Ieva, R. & Bernstein, H. D. Interaction of an autotransporter passenger domain with BamA during its translocation across the bacterial outer membrane. *Proc. Natl Acad. Sci. USA* **106**, 19120–19125 (2009).
116. Oomen, C. J. *et al.* Structure of the translocator domain of a bacterial autotransporter. *EMBO J.* **23**, 1257–1266 (2004).
117. van den Berg, B. Crystal structure of a full-length autotransporter. *J. Mol. Biol.* **396**, 627–633 (2010). **This article defines the first atomic structure of a full-length autotransporter, including both the translocator and passenger domains.**
118. Meng, G., Surana, N. K., St Geme, J. W. & Waksman, G. Structure of the outer membrane translocator domain of the *Haemophilus influenza*e Hia trimeric autotransporter. *EMBO J.* **25**, 2297–2304 (2006).
119. Ieva, R., Skillman, K. M. & Bernstein, H. D. Incorporation of a polypeptide segment into the β-domain pore during the assembly of a bacterial autotransporter. *Mol. Microbiol.* **67**, 188–201 (2008).
120. Skillman, K. M., Barnard, T. J., Peterson, J. H., Ghirlando, R. & Bernstein, H. D. Efficient secretion of a folded protein domain by a monomeric bacterial autotransporter. *Mol. Microbiol.* **58**, 945–958 (2005).
121. Pavlova, O., Peterson, J. H., Ieva, R. & Bernstein, H. D. Mechanistic link between β barrel assembly and the initiation of autotransporter secretion. *Proc. Natl Acad. Sci. USA* **110**, E938–E947 (2013).
122. Selkrig, J. *et al.* Discovery of an archetypal protein transport system in bacterial outer membranes. *Nature Struct. Mol. Biol.* **19**, 506–510 (2012).
123. Gruss, F. *et al.* The structural basis of autotransporter translocation by TamA. *Nature Struct. Mol. Biol.* **20**, 1318–1320 (2013).
124. Wright, K. J., Seed, P. C. & Hultgren, S. J. Development of intracellular bacterial communities of uropathogenic *Escherichia coli* depends on type 1 pili. *Cell. Microbiol.* **9**, 2230–2241 (2007).
125. Lillington, J., Geibel, S. & Waksman, G. Reprint of "Biogenesis and adhesion of type 1 and P pili". *Biochim. Biophys. Acta* **1850**, 554–564 (2015).
126. Mu, X. Q. & Bullitt, E. Structure and assembly of P-pili: a protruding hinge region used for assembly of a bacterial adhesion filament. *Proc. Natl Acad. Sci. USA* **103**, 9861–9866 (2006).
127. Hahn, E. *et al.* Exploring the 3D molecular architecture of *Escherichia coli* type 1 pili. *J. Mol. Biol.* **323**, 845–857 (2002).
128. Choudhury, D. *et al.* X-ray structure of the FimC–FimH chaperone-adhesin complex from uropathogenic *Escherichia coli*. *Science* **285**, 1061–1066 (1999).
129. Hultgren, S. J., Normark, S. & Abraham, S. N. Chaperone-assisted assembly and molecular architecture of adhesive pili. *Annu. Rev. Microbiol.* **45**, 383–415 (1991).
130. Vetsch, M. *et al.* Pilus chaperones represent a new type of protein-folding catalyst. *Nature* **431**, 329–333 (2004).
131. Sauer, F. G. *et al.* Structural basis of chaperone function and pilus biogenesis. *Science* **285**, 1058–1061 (1999).
132. Phan, G. *et al.* Crystal structure of the FimD usher bound to its cognate FimC–FimH substrate. *Nature* **474**, 49–53 (2011). **This paper provides the first structural insight into the mechanism of pilus assembly.**
133. Geibel, S., Procko, E., Hultgren, S. J., Baker, D. & Waksman, G. Structural and energetic basis of folded-protein transport by the FimD usher. *Nature* **496**, 243–246 (2013).
134. Remaut, H. *et al.* Donor-strand exchange in chaperone-assisted pilus assembly proceeds through a concerted β strand displacement mechanism. *Mol. Cell* **22**, 831–842 (2006).
135. Verger, D., Miller, E., Remaut, H., Waksman, G. & Hultgren, S. Molecular mechanism of P pilus termination in uropathogenic *Escherichia coli*. *EMBO Rep.* **7**, 1228–1232 (2006).
136. Olsen, A., Jonsson, A. & Normark, S. Fibronectin binding mediated by a novel class of surface organelles on *Escherichia coli*. *Nature* **338**, 652–655 (1989).
137. Hammar, M., Arnqvist, A., Bian, Z., Olsen, A. & Normark, S. Expression of two *csg* operons is required for production of fibronectin- and Congo red-binding curli polymers in *Escherichia coli* K-12. *Mol. Microbiol.* **18**, 661–670 (1995).
138. Hammer, N. D. *et al.* The C-terminal repeating units of CsgB direct bacterial functional amyloid nucleation. *J. Mol. Biol.* **422**, 376–389 (2012).
139. Robinson, L. S., Ashman, E. M., Hultgren, S. J. & Chapman, M. R. Secretion of curli fibre subunits is mediated by the outer membrane-localized CsgG protein. *Mol. Microbiol.* **59**, 870–881 (2006).
140. Wang, X., Smith, D. R., Jones, J. W. & Chapman, M. R. *In vitro* polymerization of a functional *Escherichia coli* amyloid protein. *J. Biol. Chem.* **282**, 3713–3719 (2007).
141. Goyal, P. *et al.* Structural and mechanistic insights into the bacterial amyloid secretion channel CsgG. *Nature* **516**, 250–253 (2014). **This study provides the first structure of the translocation channel in the curli system.**
142. Takagi, F., Koga, N. & Takada, S. How protein thermodynamics and folding mechanisms are altered by the chaperonin cage: molecular simulations. *Proc. Natl Acad. Sci. USA* **100**, 11367–11372 (2003).
143. Brinker, A. *et al.* Dual function of protein confinement in chaperonin-assisted protein folding. *Cell* **107**, 223–233 (2001).
144. Nenninger, A. A., Robinson, L. S. & Hultgren, S. J. Localized and efficient curli nucleation requires the chaperone-like amyloid assembly protein CsgF. *Proc. Natl Acad. Sci. USA* **106**, 900–905 (2009).
145. Hodgkinson, J. L. *et al.* Three-dimensional reconstruction of the *Shigella* T3SS transmembrane regions reveals 12-fold symmetry and novel features throughout. *Nature Struct. Mol. Biol.* **16**, 477–485 (2009).
146. Leake, M. C. *et al.* Stoichiometry and turnover in single, functioning membrane protein complexes. *Nature* **443**, 355–358 (2006).
147. Knowles, T. J., Scott-Tucker, A., Overduin, M. & Henderson, I. R. Membrane protein architects: the role of the BAM complex in outer membrane protein assembly. *Nature Rev. Microbiol.* **7**, 206–214 (2009).
148. Palomino, C., Marin, E. & Fernandez, L. A. The fimbrial usher FimD follows the SurA–BamB pathway for its assembly in the outer membrane of *Escherichia coli*. *J. Bacteriol.* **193**, 5222–5230 (2011).
149. Chen, J., Lu, G., Lin, J., Davidson, A. L. & Quiocho, F. A. A tweezers-like motion of the ATP-binding cassette dimer in an ABC transport cycle. *Mol. Cell* **12**, 651–661 (2003).
150. Yamagata, A. & Tainer, J. A. Hexameric structures of the archaeal secretion ATPase GspE and implications for a universal secretion mechanism. *EMBO J.* **26**, 878–890 (2007).
151. Lu, C., Korotkov, K. V. & Hol, W. G. Crystal structure of the full-length ATPase GspE from the *Vibrio vulnificus* type II secretion system in complex with the cytoplasmic domain of GspL. *J. Struct. Biol.* **187**, 223–235 (2014).
152. Zarivach, R., Vuckovic, M., Deng, W., Finlay, B. B. & Strynadka, N. C. Structural analysis of a prototypical ATPase from the type III secretion system. *Nature Struct. Mol. Biol.* **14**, 131–137 (2007).
153. Yeo, H. J., Savvides, S. N., Herr, A. B., Lanka, E. & Waksman, G. Crystal structure of the hexameric traffic ATPase of the *Helicobacter pylori* type IV secretion system. *Mol. Cell* **6**, 1461–1472 (2000).
154. Steadman, D., Lo, A., Waksman, G. & Remaut, H. Bacterial surface appendages as targets for novel antibacterial therapeutics. *Future Microbiol.* **9**, 887–900 (2014).
155. Ruer, S., Pinotsis, N., Steadman, D., Waksman, G. & Remaut, H. Virulence-targeted antibacterials: concept, promise, and susceptibility to resistance mechanisms. *Chem. Biol. Drug Des.* http://dx.doi.org/10.1111/cbdd.12517 (2015).
156. Houben, E. N., Korotkov, K. V. & Bitter, W. Take five — type VII secretion systems of *Mycobacteria*. *Biochim. Biophys. Acta* **1843**, 1707–1716 (2014).
157. Stanley, S. A., Raghavan, S., Hwang, W. W. & Cox, J. S. Acute infection and macrophage subversion by *Mycobacterium tuberculosis* require a specialized secretion system. *Proc. Natl Acad. Sci. USA* **100**, 13001–13006 (2003).
158. Solomonson, M. *et al.* Structure of the mycosin-1 protease from the mycobacterial ESX-1 protein type VII secretion system. *J. Biol. Chem.* **288**, 17782–17790 (2013).
159. Korotkova, N. *et al.* Structure of the *Mycobacterium tuberculosis* type VII secretion system chaperone $EspG_5$ in complex with PE25–PPE41 dimer. *Mol. Microbiol.* **94**, 367–384 (2014).
160. Cegelski, L. *et al.* Small-molecule inhibitors target *Escherichia coli* amyloid biogenesis and biofilm formation. *Nature Chem. Biol.* **5**, 913–919 (2009).
161. Duncan, M. C., Linington, R. G. & Auerbuch, V. Chemical inhibitors of the type three secretion system: disarming bacterial pathogens. *Antimicrob. Agents Chemother.* **56**, 5433–5441 (2012).
162. Paschos, A. *et al.* An *in vivo* high-throughput screening approach targeting the type IV secretion system component VirB8 identified inhibitors of *Brucella abortus* 2308 proliferation. *Infect. Immun.* **79**, 1033–1043 (2011).
163. Brinton, C. C. Jr. Non-flagellar appendages of bacteria. *Nature* **183**, 782–786 (1959).
164. d'Enfert, C., Ryter, A. & Pugsley, A. P. Cloning and expression in *Escherichia coli* of the *Klebsiella pneumoniae* genes for production, surface localization and secretion of the lipoprotein pullulanase. *EMBO J.* **6**, 3531–3538 (1987).
165. Galān, J. E. & Curtiss, R. Cloning and molecular characterization of genes whose products allow *Salmonella typhimurium* to penetrate tissue culture cells. *Proc. Natl Acad. Sci. USA* **86**, 6383–6387 (1989).
166. Koronakis, V., Sharff, A., Koronakis, E., Luisi, B. & Hughes, C. Crystal structure of the bacterial membrane protein TolC central to multidrug efflux and protein export. *Nature* **405**, 914–919 (2000).
167. Kuldau, G. A., De Vos, G., Owen, J., McCaffrey, G. & Zambryski, P. The *virB* operon of *Agrobacterium tumefaciens* pTiC58 encodes 11 open reading frames. *Mol. Gen. Genet.* **221**, 256–266 (1990).
168. Ma, D. *et al.* Molecular cloning and characterization of *acrA* and *acrE* genes of *Escherichia coli*. *J. Bacteriol.* **175**, 6299–6313 (1993).
169. Welch, R. A., Dellinger, E. P., Minshew, B. & Falkow, S. Haemolysin contributes to virulence of extra-intestinal *E. coli* infections. *Nature* **294**, 665–667 (1981).
170. Pohlner, J., Halter, R., Beyreuther, K. & Meyer, T. F. Gene structure and extracellular secretion of *Neisseria gonorrhoeae* IgA protease. *Nature* **325**, 458–462 (1987).
171. Korotkov, K. V. & Hol, W. G. Structure of the GspK–GspI–GspJ complex from the enterotoxigenic *Escherichia coli* type 2 secretion system. *Nature Struct. Mol. Biol.* **15**, 462–468 (2008).
172. Lederberg, J. & Tatum, E. L. Gene recombination in *Escherichia coli*. *Nature* **158**, 558 (1946).

Acknowledgements
The authors thank T. Marlovits for providing an EM map with a longer T3SS needle and W. G. J. Hol for the constructed dodecameric ring of the GspD cytoplasmic domains. This work was funded by Wellcome Trust grant 098302 and ERC grant 321630 to G.W. The authors apologize for the omission of some studies owing to space constraints.

Competing interests statement
The authors declare no competing interests.

DATABASES
EMDB: http://www.ebi.ac.uk/pdbe/emdb/
EMD-5915 | EMD-1763 | EMD-1875 | EMD-2567 | EMD-2524 | EMD-2750
PDB: http://www.rcsb.org/pdb/home/home.do
2XMN | 2F1M | 4CDI | 4AYT | 3EZJ | 3QSS | 2W7V | 2BH1 | 1UV7 | 3C1Q | 4KSR | 3G20 | 4DO9 | 3CI0 | 3J1W | 2Y9J | 2Y9K | 2LPZ | 4AG5 | 3JQO | 3ZBJ | 3RX9 | 3U66 | 4JIV | 4HKH | 3ZRJ | 3KVN | 4J3O | 4DWH | 4UV3 | 2Y2Y

ALL LINKS ARE ACTIVE IN THE ONLINE PDF